AN ANALYSIS OF STEADY ASYMMETRIC VORTEX SHEDDING FROM A MISSILE AT HIGH ANGLES OF ATTACK

John S. Kubin

Air Force Institute of Technology

Prepared for:

Air Force Flight Dynamics Laboratory

November 1973

Unclassified

Security Classification

AD774390

DOCUMENT CONTROL DATA - R & D

(Security classification of title, body of abstract and indexing annotation must be entered when the overall report is classified)

1. ORIGINATING ACTIVITY (Corporate author)

Air Force Institute of Technology (AFIT-EN)
Wright-Patterson AFB, Ohio 45433

2a. REPORT SECURITY CLASSIFICATION

Unclassified

2b. GROUP

3. REPORT TITLE

An Analysis of Steady Asymmetric Vortex Shedding From a Missile at High Angles of Attack

4. DESCRIPTIVE NOTES (Type of report and inclusive dates)

AFIT thesis

5. AUTHOR(S) (First name, middle initial, last name)

John S. Kubin
Major USAF

6. REPORT DATE	7a. TOTAL NO. OF PAGES	7b. NO. OF REFS
December 1973	52 64	14

8a. CONTRACT OR GRANT NO.	9a. ORIGINATOR'S REPORT NUMBER(S)
b. PROJECT NO.	GAM/AE/73A-13
c.	9b. OTHER REPORT NO(S) (Any other numbers that may be assigned this report)
d.	

10. DISTRIBUTION STATEMENT

Approved for public release; distribution unlimited.

11. SUPPLEMENTARY NOTES	12. SPONSORING MILITARY ACTIVITY
Approved for public release; IAW AFR 190-17 JERRY C. HIX, Captain, USAF Director of Information	Air Force Flight Dynamics Laboratory Wright-Patterson AFB, Ohio AFFDL/FGC

13. ABSTRACT

Recent developments of highly maneuverable missiles capable of operating at high angles of attack have shown that large unexpected side forces and yawing moments occur due to asymmetric vortex separation from a slender missile body. The objective of this report was to develop a mathematical model which accounted for the viscous effects of the boundary layer fluid that sheds as discrete vortices, and to predict the forces and moments on a missile.

An aerodynamic model in the crossflow plane based on von Karman's vortex street theory was developed. The number of vortex filaments which were shed and the positions of the filaments where determined from experimental data as a function of the crossflow Mach number. The Strouhal number was used to relate time in the crossflow plane with time to travel along the missile.

Force and moment equations were developed using a 2-D complex potential flow field in the crossflow plane which consisted of a doublet in a free stream (crossflow velocity) and a vortex, plus its image.

These equations were used to compare transverse forces and moments with experimental data to test the mathematical theory. The trend of the normal (lift) forces was predicted; however, the trend of the side force predictions was adequate only for low Mach numbers and low missile fineness ratios.

FORM 1473

14. KEY WORDS	LINK A		LINK B		LINK C	
	ROLE	WT	ROLE	WT	ROLE	WT
Missile Aerodynamics						
Missiles at High Angles of Attack						
Side Forces and Yawing Moments on Slender Bodies						
Spacing, Position, and Strength of Vortices						
Symmetric and Asymmetric Vortex Separation						
Viscous Effects Over Slender Inclined Bodies						

AN ANALYSIS OF STEADY ASYMMETRIC VORTEX SHEDDING FROM A MISSILE AT HIGH ANGLES OF ATTACK

THESIS

GAM/AE/73A-13

John S. Kubin
Major USAF

Approved for public release; distribution unlimited

AN ANALYSIS OF STEADY ASYMMETRIC VORTEX SHEDDING FROM A MISSILE AT HIGH ANGLES OF ATTACK

THESIS

Presented to the Faculty of the School of Engineering
of the Air Force Institute of Technology

Air University

in Partial Fulfillment of the
Requirements for the Degree of

Master of Science

by

John S. Kubin
Major USAF

Graduate Aerospace-Mechanical Engineering

November 1973

Preface

The recent development of highly maneuverable missiles has prompted renewed interest in the basic aerodynamics of slender bodies of revolution. Historically, potential flow analysis has been used to analyze slender bodies to determine the associated forces and moments; however, the presence of viscosity has altered the flow characteristics dramatically. Unexpected side forces and yawing moments at high angles of attack have been observed in wind tunnel tests of slender bodied missiles.

My objective in this report was to attempt to extend the slender-body theory to relatively high angles of attack in order to predict the forces and moments induced by steady asymmetric vortex shedding on a slender missile configuration.

I wish to thank Major Carl G. Stolberg, Assistant Professor of Mechanical Engineering, Aero-Mechanical Engineering Department, for his support and guidance throughout this study. Also, I wish to express my gratitude to Mr. Robert C. Nelson, Stability and Control Prediction Methods Group, Air Force Flight Dynamics Laboratory, for his assistance and cooperation. Both of these men have been extremely helpful and have made this study a rewarding academic experience for me. Finally, I would like to thank my most gracious wife, for her patience, understanding, and cheerfulness, without which I could not have completed this study.

John S. Kubin

Contents

	Page
Preface	ii
List of Figures	iv
List of Symbols	vi
Abstract	viii
I. Introduction	1
Background	1
Objective of Study	6
II. Previous Experimental Investigations	8
Experimental Measurements	8
Schlieren Studies	9
Strouhal Number Measurements	9
Wake Traverses	10
Analysis of Schlieren Photographs	10
Strouhal Number	10
Position of Vortex Breakawey Points	11
Angle Between Vortex Lines and Body Centerline	15
Force Investigation and Measurements	15
III. Aerodynamic Model	18
Assumptions	19
Aerodynamic Flow Field	20
Starting Positions of the Vortex Lines	20
Strength of the Vortex Lines	22
Calculation Procedures	24
Force and Moment Equations	26
Transverse Force Equations	27
Moment Equations	30
IV. Comparison of Results	32
V. Conclusions	48
VI. Recommendations	50
Bibliography	51
Vita	52

List of Figures

Figure		Page
1	Flow Separation on a Slender Body at High Angles of Attack..	2
2	Sketch of Wake from Slender Cone-Cylinder at Large Angles of Attack.....	4
3	Different Crossflow Regimes at Various Angles of Attack.....	5
4	Crossflow Strouhal No. Variation with Crossflow Mach No. ...	12
5	Starting Position of all Vortices in the Wake at Subcritical Reynolds Numbers.....	13
6	Vortex Starting Position as Function of Crossflow Mach No. at Supercritical Reynolds Numbers.....	14
7	Variation in Wake Parameter with Crossflow Mach No.	16
8	Slender Body Model.....	21
9	Vortex Strength Parameter as Function of Crossflow Mach No..	25
10	Crossflow Plane.....	27
11	Ogive-Missile Configuration from Pick.....	35
12	Ogive-Missile Configuration from Krouse.....	35
13	Ogive-Missile Configuration from the Air Force Flight Dynamics Laboratory.....	36
14	Model #1. Side Force Coefficient Vs Angle of Attack for Free Stream Mach No. = 0.5	37
15	Model #1. Side Force Coefficient Vs Angle of Attack for Free Stream Mach No. = 0.6	38
16	Model #2. Side Force Coefficient Vs Angle of Attack for Free Stream Mach No. = 0.6	39
17	Model #2. Side Force Coefficient Vs Angle of Attack for Free Stream Mach No. = 0.9	40
18	Model #3. Absolute Side Force Coefficient Divided by the Lift Coefficient Vs Angle of Attack for Free Stream Mach No. = 0.55	41

Figure		Page
19	Model #4. Side Force Coefficient Vs Angle of Attack for Free Stream Mach No. = 0.6	42
20	Model #4. Side Force Coefficient Vs Angle of Attack for Two Different Starting Positions for the Vortex Filaments at Free Stream Mach No. = 0.85	43
21	Model #5. Side Force Coefficient Vs Angle of Attack for Free Stream Mach No. = 0.6	44
22	Model #2. Normal Force Coefficient Vs Angle of Attack for Free Stream Mach No. = 0.6	45
23	Model #2. Normal Force Coefficient Vs Angle of Attack for Free Stream Mach No. = 0.9	46
24	Model #5. Normal Force Coefficient Vs Angle of Attack for Free Stream Mach No. = 0.6	47

List of Symbols

α	Angle of Attack
χ	Wake Parameter, $\tan \xi / \tan \alpha$
C_M	Pitching Moment Coefficient
C_N	Yaw Moment Coefficient
C_n	Normal Force Coefficient
C_y	Side Force Coefficient
d	Equivalent Body Diameter
δ	Complex Angle Measured Counterclockwise from the Y (real) Axis
$\bar{F}$	Total Transverse Force
FR	Missile Fineness Ratio
$d\bar{F}/dX$	Force per Unit Length Acting on the Body Cross Section
Γ	Vortex Circulation
g'	Distance Between Breakaway Points of Consecutive Vortex Lines Measured Along the Missile Body
$\Gamma/V\ d\ \sin \alpha$	Nondimensional Vortex Strength
h	Spacing Between Infinite Parallel Rows of a von Karman Vortex Street
l	Distance Apart of Vortices of Like Sign
l_s	Distance Apart of Vortices of Like Sign Measured Normal to the Vortex Line
M_c	Crossflow Mach Number
n	Cycles per Second
ϕ	Perturbation Potential in the σ Plane
ψ	Stream Function
R	Missile Radius
r, δ	Polar Coordinates; $Y = r \cos \delta$, $Z = r \sin \delta$

r	Radius Vector in Y, Z Plane
ρ	Mass Density of Fluid
S	Strouhal Number
σ	Complex Crossflow Plane
t	Time in X, Y, Z System
U	Velocity of the Cylinder Relative to the Free Stream
U_s	Induced Transport Velocity Normal to the Vortex Lines
V	Free Stream Velocity
ν	Kinematic Viscosity
$w(\sigma)$	Complex Potential
X	Longitudinal Distance in X, Y, Z System
ξ	Angle Between the Body Centerline and the Path Traced by the Shed Vortex Filament
Y	Real Axis in σ Plane
$\bar{Y}$	Side Force Along Y Axis
Z	Imaginary Axis in σ Plane
$\bar{Z}$	Normal Force Along Z Axis, Lift
$\bar{\zeta}$	Momentum Vector

Abstract

Recent developments of highly maneuverable missiles capable of operating at high angles of attack have shown that large unexpected side forces and yawing moments occur due to asymmetric vortex separation from a slender missile body. The objective of this report was to develop a mathematical model which accounted for the viscous effects of the boundary layer fluid that sheds as discrete vortices, and to predict the forces and moments on a missile.

An aerodynamic model in the crossflow plane based on von Karman's vortex street theory was developed. The number of vortex filaments which were shed and the positions of the filaments were determined from experimental data as a function of the crossflow Mach number. The Strouhal number was used to relate time in the crossflow plane with time to travel along the missile.

Force and moment equations were developed using a 2-D complex potential flow field in the crossflow plane which consisted of a doublet in a free stream (crossflow velocity) and a vortex, plus its image.

These equations were used to compare transverse forces and moments with experimental data to test the mathematical theory. The trend of the normal (lift) forces was predicted; however, the trend of the side force predictions was adequate only for low Mach numbers and low missile fineness ratios.

AN ANALYSIS OF STEADY ASYMMETRIC VORTEX SHEDDING FROM A MISSILE AT HIGH ANGLES OF ATTACK

I. Introduction

Background

The Air Force and Navy are currently developing highly maneuverable missiles capable of operating at high angles of attack. This development has prompted renewed interest in the basic aerodynamics of slender bodies of revolution. These early flight vehicles flew relatively straight trajectories at low angles of attack; consequently, their aerodynamic performance was predictable through the use of potential flow analysis (Ref 4:2). Potential flow theory was based upon inviscid, incompressible flow, which predicts the lifting forces on a slender body at low angles of attack and can be extended to moderate supersonic speeds.

It was recognized by early investigators that an attempt to extend potential flow analysis beyond small angles of attack would require consideration of viscosity and would drastically alter the flow characteristics. The way viscosity alters the flow regime is illustrated in Fig 1. Boundary layer separation causes an adverse crossflow pressure gradient on the lee side of the body, and the boundary layer fluid "rolls up" into two cores of concentrated vorticity. The low pressures produced on the lee side of the missile increase the lift and drag forces above those values predicted by the linear potential theories (Ref 4:2).

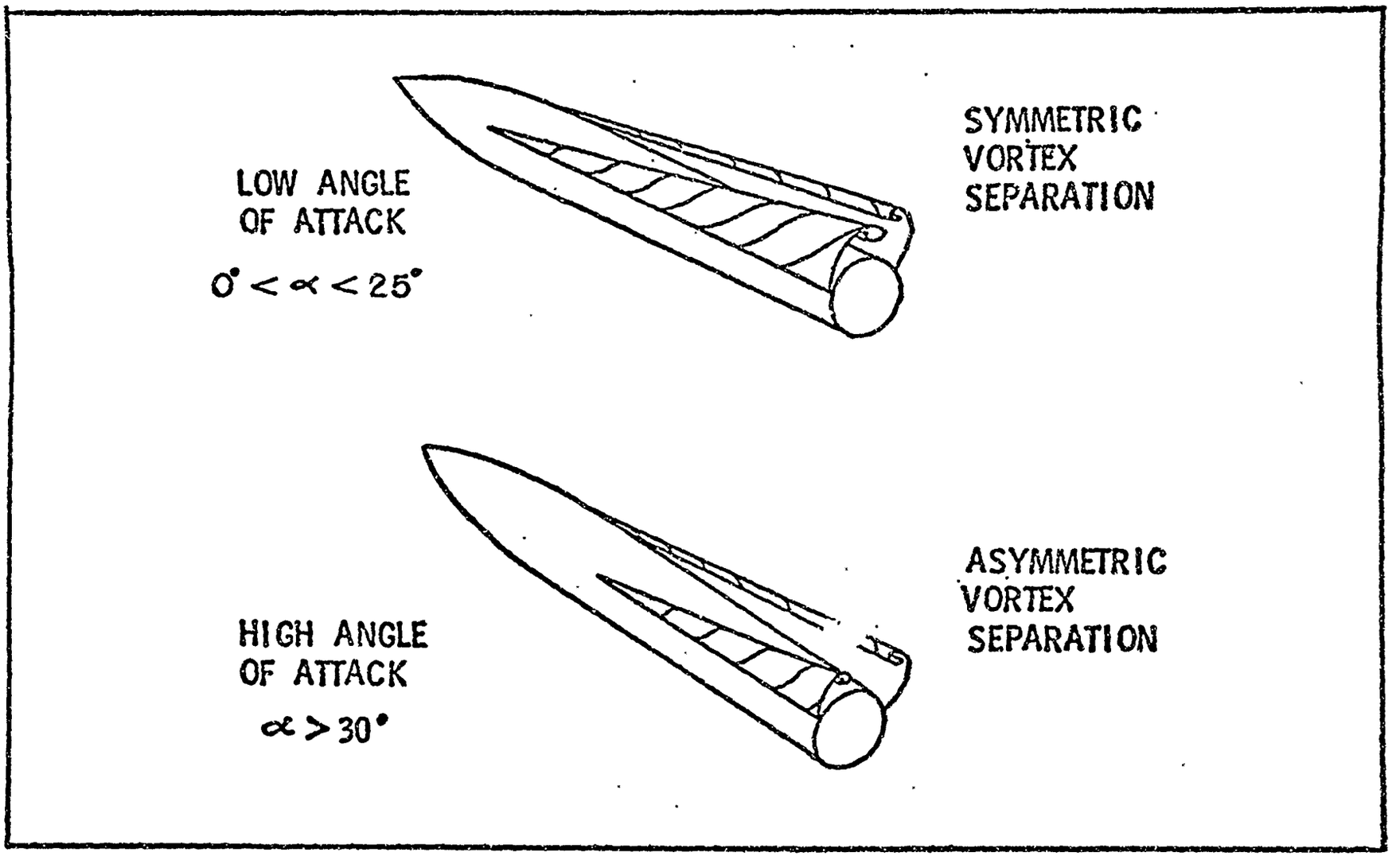

Fig. 1. Flow Separation on a Slender Body at High Angles of Attack

This problem, which has plagued the Air Force and Navy during the recent development of highly maneuverable missiles, is due to the large unexpected forces and moments that occur at high angles of attack. These forces and yawing moments were initially observed with the missile mounted at zero sideslip during wind tunnel tests at high angles of attack. It was initially assumed that turbulent flow in the wind tunnel or possible missile misalignment was the cause of these forces. It was subsequently determined from tunnel tests that asymmetric shedding of vortices from the body caused these unexpected forces. This shedding can be symmetrical or asymmetrical, as well as steady or unsteady.

For crossflow over a cylinder, the vortices on the lee side of the cylinder form from the separated boundary layer fluid. The pattern of these vortices behind the cylinder is dependent on the Reynolds number (Ref 6). The wake behind a missile is similar to the wake which develops behind a two-dimensional cylinder as viewed in successive crossflow planes along the missile. Initially, as shown in Section A of Fig 2, a pair of vortex sheets are formed which then roll up into a pair of vortex lines. At later cross sections, as shown in Section B of Fig 2, only a single vortex sheet is formed which rolls up into a vortex line near the body. The previous rolled up vortex sheets appear as vortex lines in an asymmetrical pattern behind the missile.

The pattern of the vortex filaments (symmetric, asymmetric) primarily depends upon the crossflow Reynolds number, while the nose shape, nose fineness, and overall fineness ratio have a minor influence on the vortex filament pattern. At high angles of attack and high crossflow Mach

numbers, the vortex filaments which trail behind the missile appear in the crossflow plane to be similar to a von Karman vortex street (Ref 9: 377-384).

In general, the vortex pattern can be described by four separate flow regimes as shown in Fig 3. At angles of attack from 5 to 25 degrees, a symmetric vortex pair is shed; consequently, no side forces exist. Beyond 25 degrees angle of attack, the vortex cores become asymmetric and alternately discharge from the missile body. It has been shown experimentally that when asymmetrical vortices exist, considerable side force and yawing moments are produced, especially at subsonic speeds. The asymmetric vortex pattern remains steady until an angle of attack of 50-70 degrees. Here, the asymmetric pattern becomes unsteady and alternates back and forth. Above 70 degrees angle of attack, the flow pattern degenerates into a completely turbulent wake.

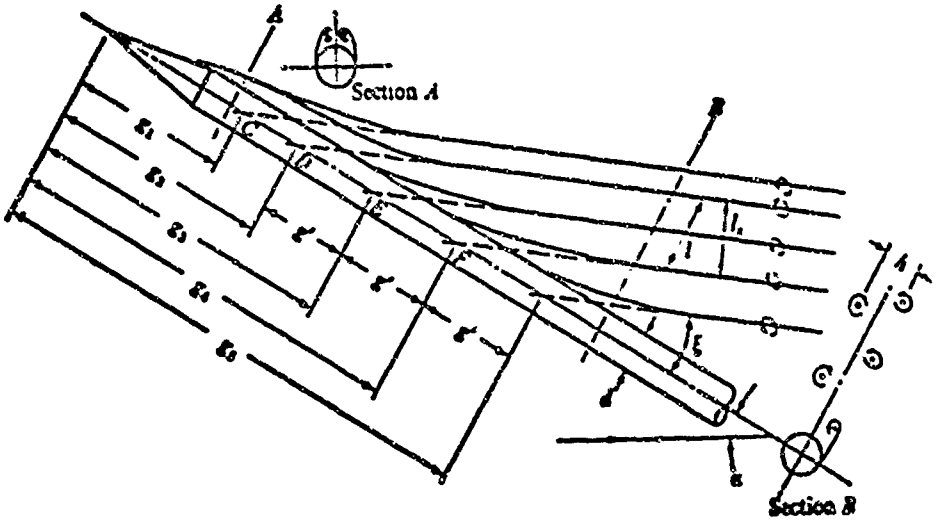

Fig 2. Sketch of Wake from Slender Cone-Cylinder at Large Angle of Attack (Ref 13:752).

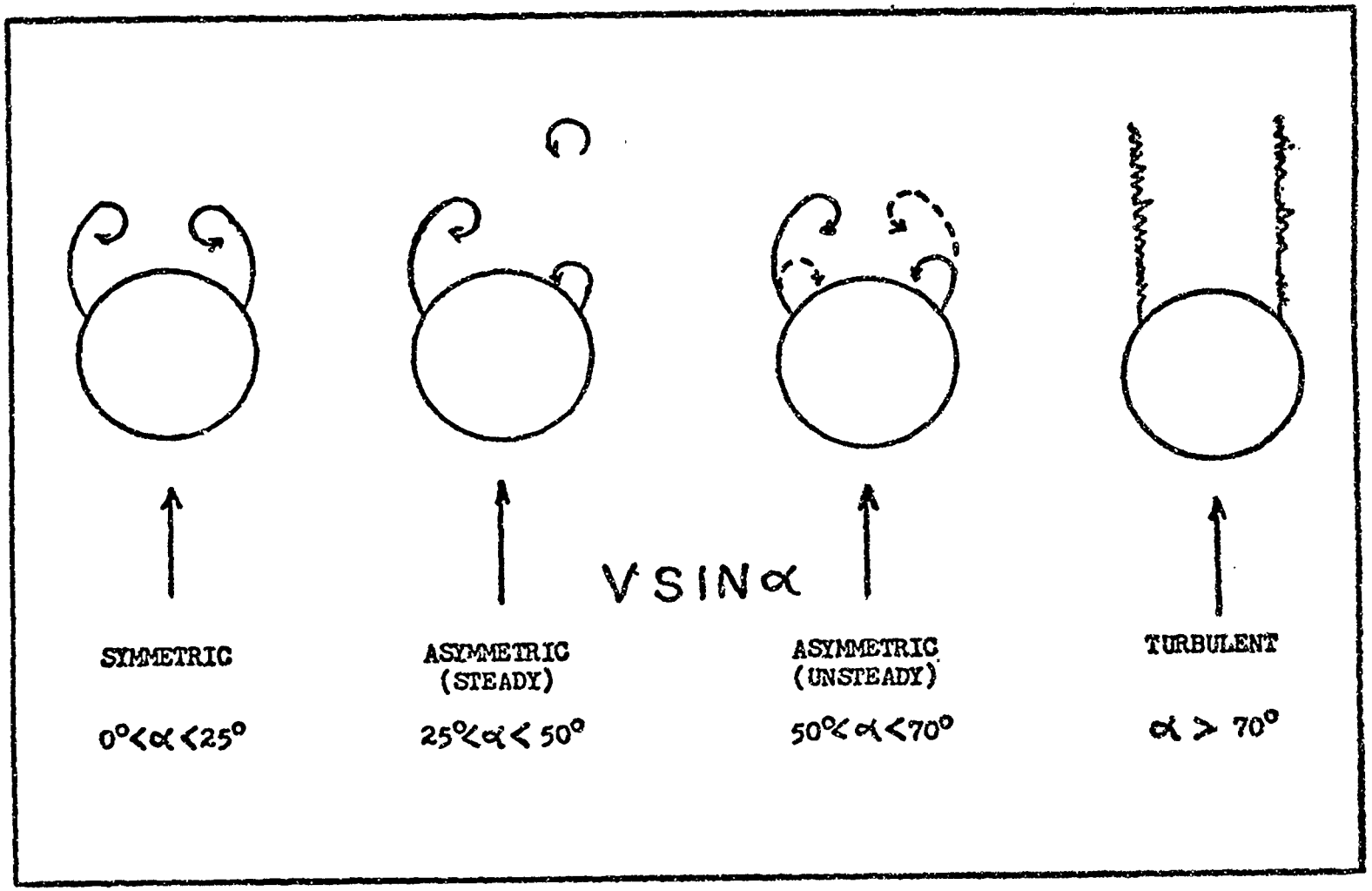

Fig. 3. Different Crossflow Regimes at Various Angles of Attack

Potential theory has been used with some success for angles of attack up to about 14 degrees. There are several analytical techniques which give reasonable results for the case of steady symmetric vortex shedding, but almost no work has been done in the area of asymmetric vortices. A calculating technique for asymmetrical loading must be developed in order to be able to design missiles that will be capable of maneuvering at high angles of attack (Ref 4:4).

Objective of Study

The objective of this study is to develop an analytical method for calculating the side force and yawing moment on a missile at high angles of attack for the case of steady asymmetric vortex shedding. The method also should be capable of calculating the normal force and the pitching moment on a missile for the same flow regime.

The missile configuration studied will be a cone-cylinder of high fineness ratio without fins attached to the missile. Even though the nose shape has an effect upon the magnitude of the side force coefficient, no attempt will be made to vary the nose fineness ratio and/or bluntness.

The flow field model used for the missile is the potential flow model for slender bodies with the addition of discrete vortices. Using the method of matched asymptotic expansion, one can show that the potential flow field can be divided into an inner and outer part (Ref 2:107-113). As a consequence of the expansions (or the equivalence rule) one can also show that for a general slender body, only the inner flow is needed to calculate the transverse forces and moments. The inner flow is a constant density two-dimensional crossflow around a cylinder, and is independent of the Mach number. In this report, the crossflow velocity has been non-dimensionalized and is referred to as crossflow Mach number.

The potential flow used to model the crossflow plane is that of an expanding cylinder with the addition of discrete vortices. The discrete vortices are introduced to model the viscous effect of the boundary layer fluid being shed from the cylinder as the vortex sheets which roll up into line vortices.

The succeeding section describes previous experimental and theoretical efforts in the symmetrical and asymmetrical vortex shedding regimes.

II. Previous Experimental Investigations

Thomson and Morrison performed extensive schlieren studies and yawmeter traverses of the wake behind a slender cone-cylinder of high fineness ratio (greater than 25) at large angles of attack (Ref 13:751). They were able to determine the number of vortex filaments shed, the starting positions, and the circulation strength, as a function of the crossflow Mach number.

Thomson and Morrison have proposed a simple flow model for describing the asymmetrical wake pattern in incompressible flow. The flow model is based on a combination of von Karman's vortex street theory and the impulse flow analogy for describing the asymmetrical wake pattern. This model implies that the angle between the body centerline and the paths traced by the shed vortex filament can be used to determine the vortex strength, while the spacing of the vortex lines is a measure of the Strouhal number of the wake for a circular cylinder with the same crossflow conditions. The flow model was deduced from experimental data obtained by Thomson and Morrison in their earlier tests; however, the method could not account for compressibility. The authors have performed additional experiments to measure the crossflow Strouhal number, vortex strength, and vortex starting positions in the wake from a slender cone-cylinder at angles of attack over a wide range of flow conditions (Ref 14:1-16).

Experimental Measurements

Thomson and Morrison were able to show from schlieren studies and yawmeter traverses that the wake behind a slender missile at varying angles of attack was generally steady for the asymmetric vortex pattern

they investigated. However, under certain conditions, the wake exhibited an instability. They reported that pitot pressure plots were used to give them information on the growth of the wake vortices, and the results of the yawmeter traverses were used to obtain vortex strengths to compare with the values deduced from the schlieren study and flow model (Ref 14:1). All of their experiments were conducted at crossflow Reynolds numbers in the subcritical ($\leq 7.5 \times 10^4$) range. Pick (Ref 11) performed comparable experiments at both subcritical and supercritical Reynolds numbers for free stream Mach numbers of 0.4 to 1.1. The strength of the wake vortices was found to vary substantially with crossflow Mach number. Von Karman's vortex street theory was combined with the sweepback principle to obtain estimates of the vortex strength. The wake was analyzed by the use of schlieren photographs by means of the impulse flow analogy and by considering the vortex filaments as part of a yawed infinite vortex street.

Schlieren Studies. Allen and Perkins (Ref 1) found that a vortex line becomes visible when viewed in a standard schlieren system. The vortex center can be observed as a boundary of regions of low and high light intensity which results from the change of sign of the density gradient at the center of the vortex. Fig 2 illustrates the vortex line positions behind the missile as determined by analysis of the schlieren photographs. The vortex lines are straight except for a small portion next to the missile body.

Strouhal Number Measurements. The Strouhal number was determined by observing the pressure fluctuations at a point near the upstream stagnation region of a cylinder mounted normal to the flow by the use of a

piezo-electric transducer. The frequency of the pressure fluctuation is identical with the frequency of vortex shedding in the wake; thus, the Strouhal number can be readily obtained (Ref 14:5). These results agree quite accurately with those of Fung (Ref 5:801). Also, Thomson and Morrison determined that the Reynolds number was not a significant parameter in the Mach number range covered by these tests.

Wake Traverses. Thomson and Morrison performed six experimental investigations of the flow within the compressible wake. They also used an experiment conducted at 100 ft/sec by Griss (Ref 7) to provide data at incompressible speeds.

The pattern of vortices behind the missile can be as shown in Section B of Fig 2 or an opposite pattern (mirror image) which is primarily dependent upon the misalignment of the nose of the missile. Thomson and Morrison determined that only a slight rotation of the body about its axis could change the pattern from one vortex sequence to another. In order to preclude the alternate shedding, the missile was mounted as a fixed body and the probe was moved by the means of a separate traversing mechanism.

Analysis of Schlieren Photographs

Strouhal Number. The values of the Strouhal number have been determined by measuring values of (g'/d) from photographs and then inserting (g'/d) into the equation

$$S = \frac{d \operatorname{Tan}\alpha}{2g'} \qquad (1)$$

where S is the Strouhal number, g' is the distance between breakway points of consecutive vortices measured along the body, d is the body diameter, and α is the angle of attack.

A curve generated from data of the Strouhal number versus crossflow Mach number is shown in Fig 4. The measured value of the Strouhal number remains constant until the crossflow Mach number reaches approximately 0.7, which corresponds to the formation of shock waves on the lee side of the missile body. Then, the Strouhal number increases with increasing crossflow Mach number. The measured Strouhal number of 0.2 for crossflow Mach numbers less than 0.7 is very close to the value for a circular cylinder for subcritical Reynolds number (Ref 14:9).

Position of Vortex Breakaway Points. As mentioned earlier, the nose misalignment determines the pattern of the vortices. A few degrees rotation of the body or a slight change in angle of attack can cause the vortices to adjust from one pattern to another. Also, the entire sequence of vortices can shift slightly forward or aft along the missile; consequently, the data analysis for the breakaway points contains appreciable scatter (Ref 13:768).

The starting position of all vortices in the wake for subcritical Reynolds number is shown in Fig 5, and for supercritical Reynolds number regime in Fig 6. The analysis is based on a non-dimensional parametric representation by the rearrangement of Eq (1) which shows that the spacing between vortex cores is related to the shedding frequency of a circular cylinder in the following equation:

$$\frac{g'}{d} = \frac{0.5}{S \tan\alpha} \qquad (2)$$

Consecutive vortices are spaced apart a distance g'. One can readily observe in Fig 2 that the first two vortex filaments are influenced by the expanding portion of the nose section of the missile. Thomson and Morrison observed from schlieren photographs that the strength of the

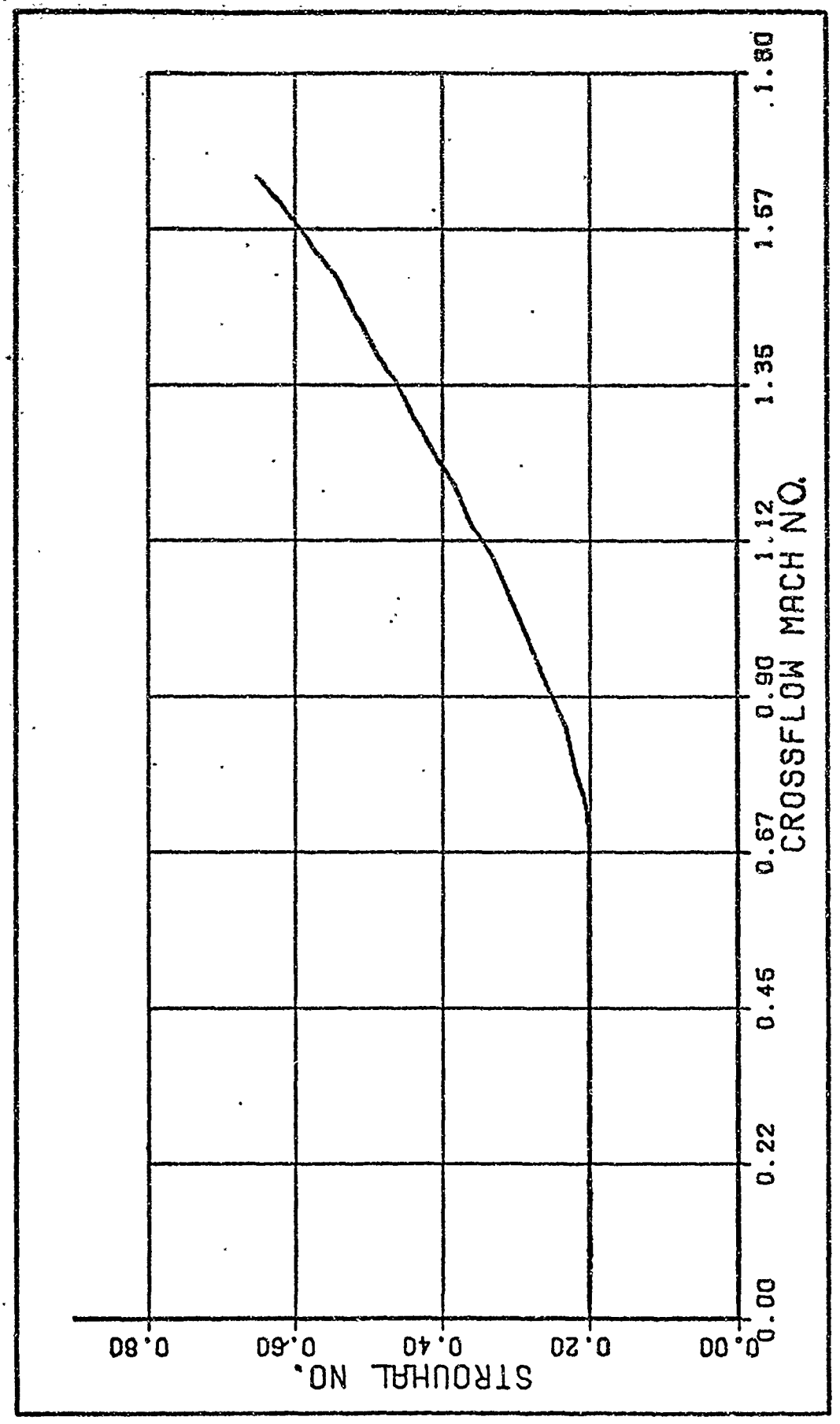

Fig. 4. Crossflow Strouhal No. Variation with Crossflow Mach No. (From Ref 13:768)

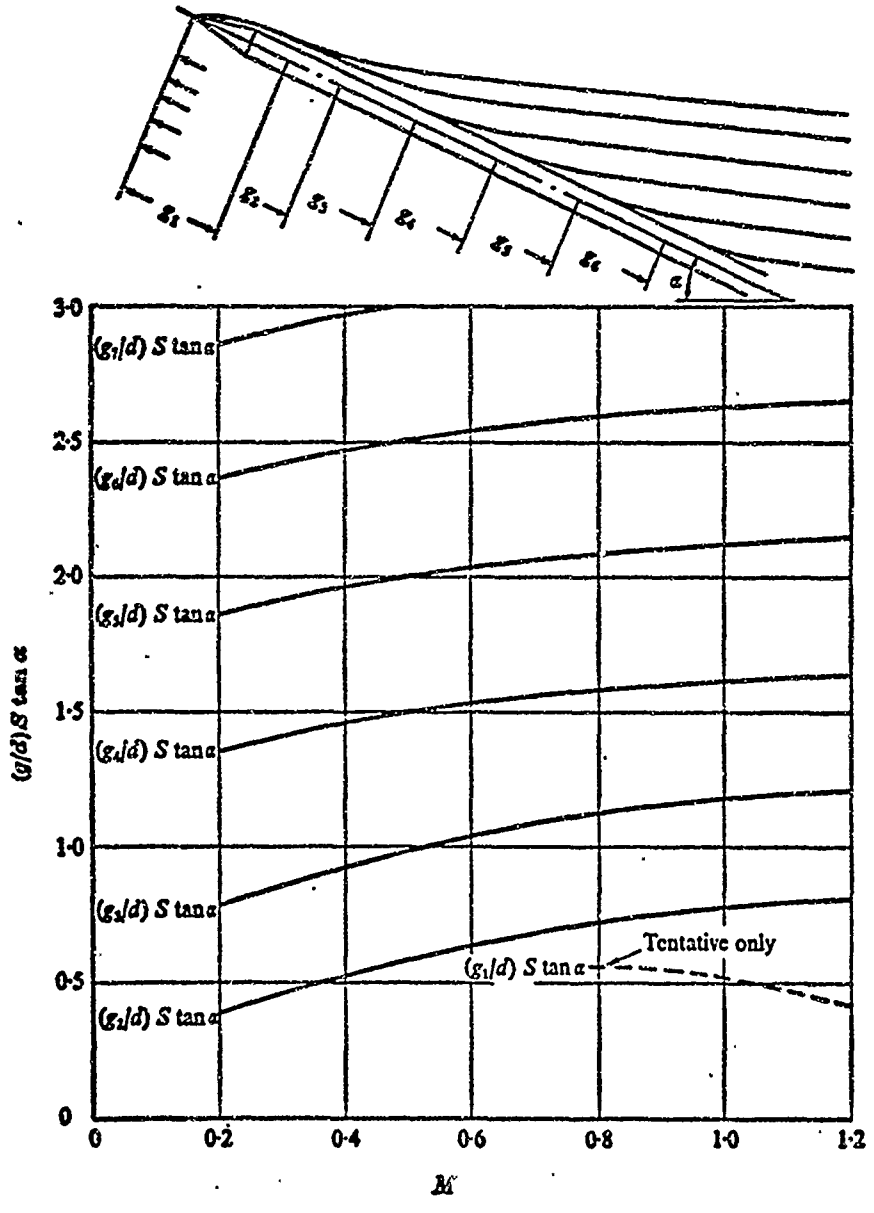

Fig. 5. Starting Position of all Vortices in the Wake at Subcritical Reynolds Numbers (From Ref 13:771)

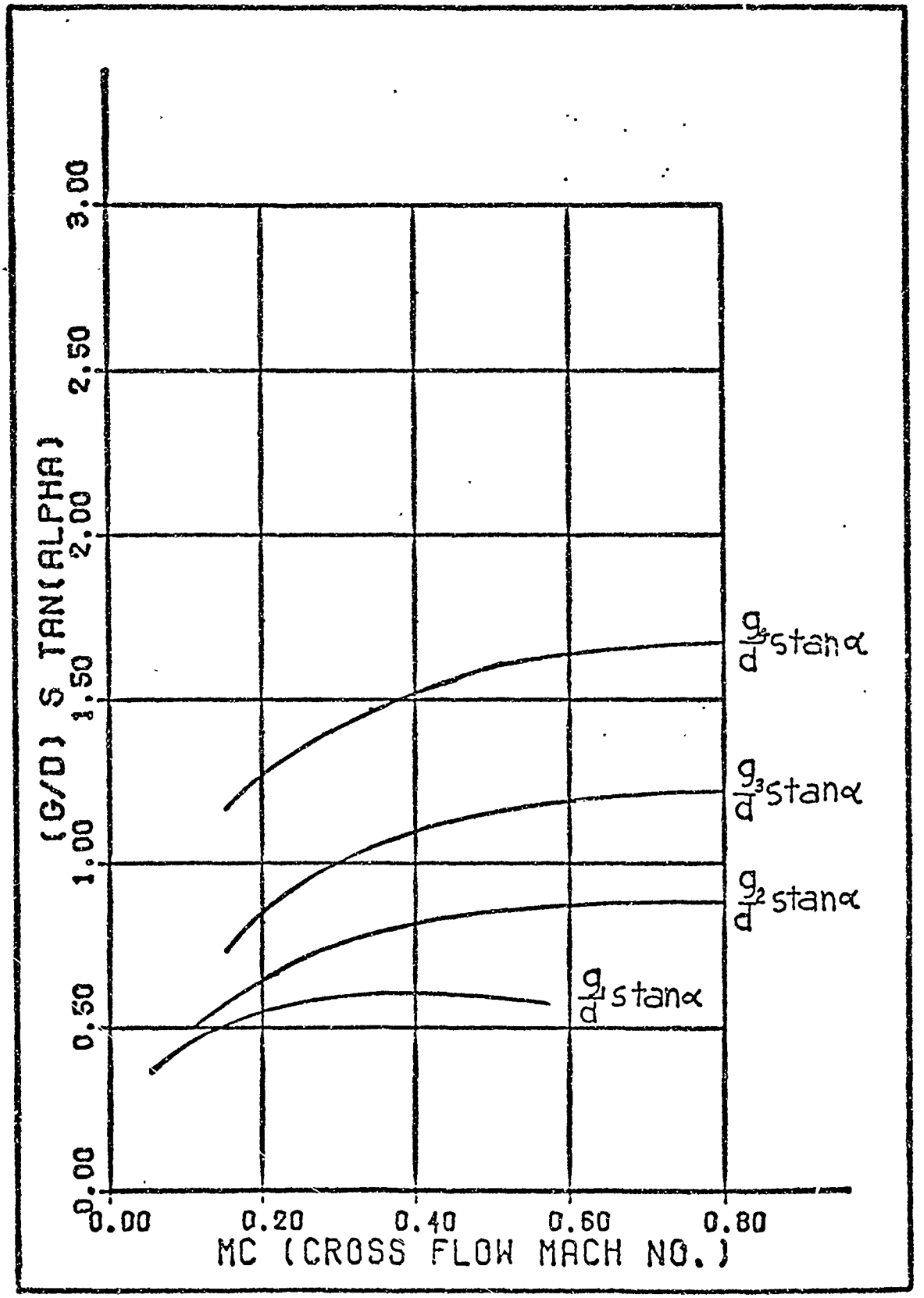

Fig. 6. Vortex Starting Position as Function of Crossflow Mach No. at Supercritical Reynolds Numbers (From Ref 14:10)

first two vortex filaments was very weak. The distance separating the third, fourth, and succeeding vortices was found to be largely independent of the nose geometry. Therefore, the spacing will be constant for the equivalent von Karman vortex filaments which originate in boundary layer fluid from the non-expanding portion of the missile body.

Angle Between Vortex Lines and Body Centerline. The angle (ξ) between the body centerline and the position of the shed vortex filaments can be determined from schlieren photographs (see Fig 2). The parameter ($\chi = \tan\xi/\tan\alpha$) can also be determined from schlieren photographs as a function of the crossflow Mach number as shown in Fig 7. The curve was generated from data, and the amount of scatter produced an error of approximately 2.5%, which is due to the difficulty of interpreting the schlieren photographs. It is readily observed that a minimum value of χ occurs in the neighborhood of $M_c = 0.75$, which corresponds to the first appearance of a shock wave.

Force Investigation and Measurements

Several techniques have been investigated which consider the actual vortex structure to determine the normal force. Bryson (Ref 3) and Schindel (Ref 12) have represented the viscous crossflow by a potential flow model in which a pair of symmetrical vortices were attached to the cylindrical cross section. They showed that the motion and strength of the vortices can be computed for the case of the impulsively-started cylinder if the separation points are known. With the aid of the impulse flow analogy, the time (t) can be replaced with $X/V\cos\alpha$; therefore, the position and strengths of the vortices can be computed for each axial station along the missile body. From this information the normal force can be determined (Ref 4:3).

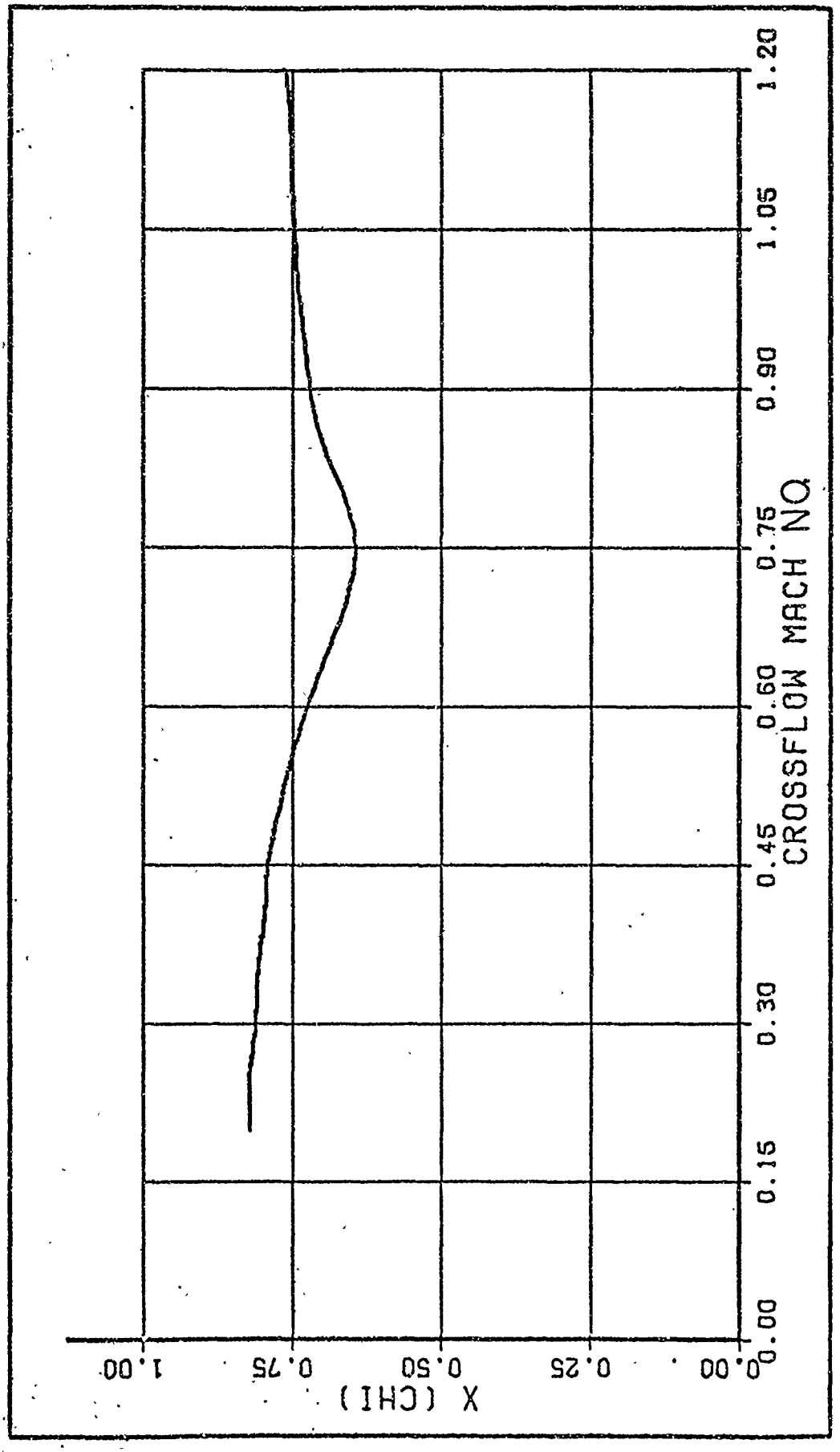

Fig. 7. Variation in Wake Parameter with Crossflow Mach No. (From Ref 13:772)

Pick (Ref 11) and Krouse (Ref 8) measured side forces associated with asymmetric vortex shedding. Additional unpublished data was obtained by the Air Force Flight Dynamics Laboratory. Krouse investigated the flow around a tangent-ogive cylinder with nose length-to-diameter ratio of 4.89 and overall fineness ratio of 10 for Mach numbers of 0.55 and 0.80 with a crossflow Reynolds number of 4.5×10^5 to 8.0×10^5. Pick conducted similar investigations for ogive-cylinders with various nose bluntnesses and overall fineness ratio of about 11, and for free stream Mach numbers from 0.5 to 1.1. Both Krouse and Pick used missile shapes of much less fineness ratio than Thomson and Morrison. Krouse measured side forces that were approximately 60 to 70 per cent of the values of the normal lift force on the missile at angles of attack between 30-40 degrees. Pick studied the effects of nose fineness and bluntness ratio on the magnitude of the side forces produced by asymmetrical flow separation on ogive-cylinder bodies. He concluded that an increase in the fineness ratio resulted in an increase in the side force, and conversely, an increase in the nose bluntness resulted in a decrease in the maximum side force. Pick concluded that the induced side forces can be dramatically reduced by generating a turbulent boundary layer, which results in delayed separation.

In the following sections an approximate flow field model will be postulated so that the position and strength of the rolled up vortex sheets may be calculated. Next, from slender body theory, the equations required to calculate the transverse forces and moments acting on the missile will be developed. Finally, the equations will be applied to calculate the forces and moments for several missile configurations and the results compared to experimental data.

III. Aerodynamic Model

Experiments by Thomson and Morrison, Pick, and others indicate that vortex separation from the body of a missile is basically a crossflow phenomenon and that its effect on the aerodynamic characteristics of a slender body can be analyzed by an inviscid model based on the approximations of slender body theory. A two-dimensional solution in the crossflow plane has been the classical analytic technique. This investigation will use an inviscid theory that is capable of evaluating the vortex-induced forces and moments on a slender axisymmetric body exhibiting steady asymmetric vortex shedding.

The wake behind the missile at high angles of attack exhibits the same behavior as that behind a two-dimensional cylinder of finite length. When a circular cylinder is suddenly accelerated from rest to a speed V in a fluid (Mach number small compared to unity), it is observed that the initial flow field is irrotational, but very soon after starting, the boundary layer separates at the rearward stagnation point. These two separation points propagate symmetrically away from the sides of the cylinder. When these boundary-layer separation points reach a certain angular distance around the sides of the cylinder, two regions of vorticity break away from the boundary layer and move downstream, beginning the formation of a wake. This description applies for Reynolds number (Re = Ud/v) greater than about 5. At lower Re no wake is formed as the flow is governed primarily by viscous forces (Stokes' flow). Further development of the wake depends on Re; for $50 < Re < 100$ an antisymmetry builds up quickly and regular eddy shedding (von Karman vortex street) begins. For $Re > 10^5$, the alternate eddy shedding begins but is rapidly superseded

by a completely turbulent flow in the wake (Ref 3). The analysis in this report is concerned with antisymmetric shedding.

Assumptions

The major assumptions used in developing the analysis are:

a. The vortex sheets roll up into vortex lines of constant strength. It has been observed that a vortex sheet that is shed from the cylinder rolls up within a distance of one diameter; consequently, it seems plausible to model the shed vortex sheet as a line of constant strength. Also, the vortex sheet that is attached to the missile will be modeled as a filament line at the edge of the vortex sheet that has the same strength as the other vortex lines.

b. It is assumed that an empirically modified vortex street analysis will properly predict the strengths and position of the rolled up vortex sheets. Since it is observed that the vortex sheets roll up in the wake of the missile and appear as stationary lines in schlieren photographs (Ref 13:784), a von Karman vortex street analysis will be used. The results of measurements from the schlieren photographs will be used in conjunction with vortex street analysis to estimate the strength and position of the rolled up vortex sheets.

c. It is assumed that even for high angles of attack, slender body theory will give approximate equations to calculate the transverse force and moments if the small angle approximation is modified by using the sine and cosine functions.

d. Compressibility effects can be neglected. The assumption of constant density will be made since slender body theory in the crossflow plane and the von Karman vortex street analysis is one of constant density.

A result of slender body theory is that the flow in the crossflow plane is independent of Mach number, and that the transverse forces and moments depend only on the flow in the crossflow plane.

Aerodynamic Flow Field

A sketch of the vortex system behind a slender cone-cylinder at an angle of attack is shown in Fig 8. The flow pattern will be analyzed by considering the vortex pattern to be a steady yawed vortex street for which vortex street theory may be applied.

Starting Positions of the Vortex Lines. The parameter for describing the periodic shedding of vortices from a circular cylinder in two dimensions is the Strouhal number (S),

$$S = \frac{nd}{U} \tag{3}$$

where n is the frequency of shedding vortices of like sign, d is the diameter of the cylinder, and U is the velocity of the cylinder relative to the free stream. Considering a cylinder yawed at an angle (α) to the free stream velocity (V), the velocity at right angles to the cylinder is

$$U = V \sin \alpha \tag{4}$$

and hence

$$S = \frac{nd}{V \sin \alpha} \tag{5}$$

In 2-D theory, 1/n represents the time interval between the instants of shedding of vortices of like sign; here the interval is taken as the time for the component of flow along the body ($V \cos \alpha$) to travel a distance 2 g'. Thus

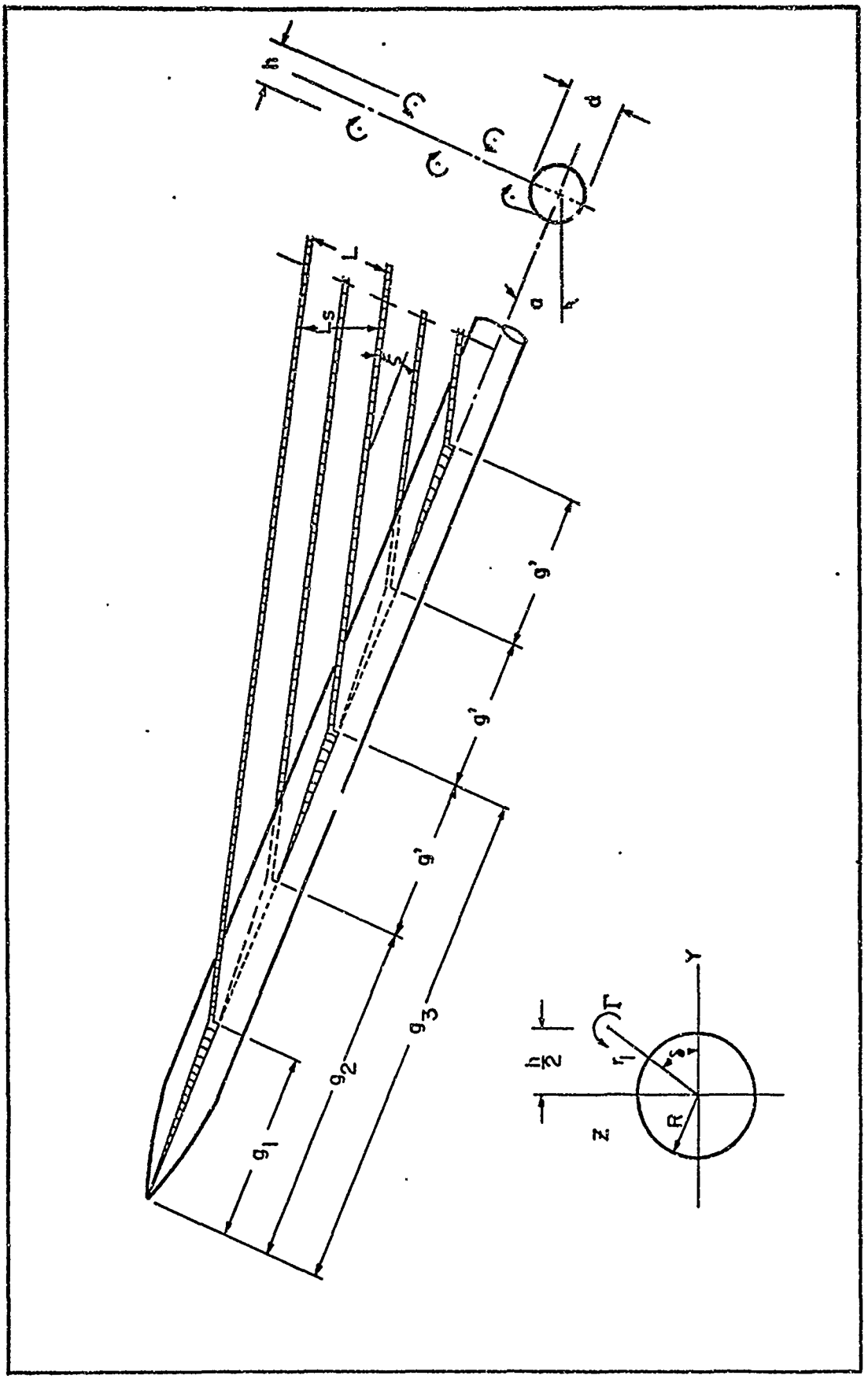

Fig. 8. Slender Body Model

$$\frac{1}{n} = \frac{d}{S V \sin\alpha} = \frac{2g'}{V\cos\alpha} \tag{6}$$

or

$$g' = \frac{d}{2S\,\mathrm{Tan}\,\alpha} \tag{7}$$

where g' is the distance between successive vortex lines.

The starting position of the vortex lines for two different experimental tests are shown for subcritical Reynolds number in Fig 5 and for supercritical Reynolds number in Fig 6 as $g_i/d\ S\ \tan\alpha$ versus the crossflow Mach number, where i = 1, 2, 3, ... i. e., (the first, second, and succeeding vortex line starting positions from the nose of the missile). Since

$$\frac{g'}{d} S\,\mathrm{Tan}\,\alpha = \frac{1}{2} \tag{8}$$

the non-dimensional distance between vortex lines should be $\frac{1}{2}$, which is approximately true for the distance between the third, fourth, and subsequent vortex lines. The starting positions of the first two vortex lines are greatly influenced by the nose shape of the missile which has an expanding diameter. Also, the fact that the first two vortex lines have a tendency to be shed as a symmetrical pair, rather than alternately, influences the starting positions. This behavior is the same as that for a cylinder in crossflow at sufficiently low Reynolds number.

Strength of the Vortex Lines. The strength of the vortex lines can be approximated by using vortex street theory. A vortex street consists of two parallel infinite rows of line vortices of uniform spacing. Alternate vortices have opposite sign; the spacing between rows in the cross

section view are shown in Fig 8. In vortex street analysis for incompressible two-dimensional flow, the self-induced transport velocity (U_s) of the vortex street normal to the vortex lines is given by

$$U_s = \frac{\Gamma}{2l_s} \tanh\left(\frac{\pi h}{l_s}\right) \tag{9}$$

where Γ is the vortex strength and l_s is the distance between vortices of like sign measured normal to the vortex lines. Theory also shows that an array of two parallel rows of vortex lines will be stable if the spacing ratio is

$$\frac{h}{l_s} = \frac{\sqrt{2}}{\pi} = 0.281 \tag{10}$$

where h is the distance between the infinite parallel rows of vortices. Since the vortex lines are stationary, the self-induced velocity U_s must be countered by the component of the free stream velocity normal to the vortex lines as follows:

$$U_s = V \sin\left(\alpha - \xi\right) \tag{11}$$

From the geometry in Fig 8, the following relations can be deduced:

$$l_s = l \cos\xi \tag{12}$$

$$\tan\xi = \frac{1}{2g'} \tag{13}$$

Equating Eqs (9) and (11) and using Eqs (10, 12, and 13) gives

$$\frac{\Gamma}{Vd\sin\alpha} = \coth\left(\sqrt{2}\right)\frac{4g'}{d}\cos^2\left(\xi\right)\tan\xi\left(1 - \frac{\tan\xi}{\tan\alpha}\right) \tag{14}$$

or upon using Eq (9)

$$\frac{\Gamma}{Vd\sin\alpha} = \coth\left(\sqrt{2}\right)\frac{2}{S}\cos^2\left(\xi\right)\frac{\tan\xi}{\tan\alpha}\left(1 - \frac{\tan\xi}{\tan\alpha}\right) \tag{15}$$

The perameter $\Gamma/V\,d\,\sin\alpha$ (nondimensional vortex strength) can be determined if the values of the Strouhal number and the angle ξ between the vortex lines and the missile are known for a given angle of attack. The value of Strouhal number as a function of the crossflow Mach number can be determined experimentally as shown in Fig 4. Also, the parameter χ as a function of the crossflow Mach number can be determined experimentally from schlieren photographs, as shown in Fig 7, where

$$\chi = \frac{\mathrm{Tan}\,\xi}{\mathrm{Tan}\,\alpha} \tag{16}$$

Using the experimental values of Strouhal number (S) and the parameter χ as a function of crossflow Mach number from Fig 7, the value of $\Gamma/V\,d\,\sin\alpha$ can be computed using Eq (15). The nondimensional vortex strength as a function of the crossflow Mach number and angle of attack is shown in Fig 9. Thomson and Morrison (Ref 13:774) displayed a similar plot of vortex strength estimated from schlieren photographs and wake traverses for a 30 degree angle of attack. It can be seen from Fig 9 that the vortex strength increases with increased crossflow Mach number (M_c) to a maximum value at 0.75, and then decreases. The peak value corresponds to a Mach range where compressibility effects begin to be significant. It is observed that as the angle of attack is increased, the magnitudes of the nondimensional vortex strength decrease in value.

Calculation Procedures. From the above aerodynamic flow field analysis, the position and the strengths of vortex filaments in the wake of a missile at a high angle of attack may be determined. For a given missile operating at a specified angle of attack and crossflow Mach number, if one proceeds according to the following steps, the position and strength of each vortex line can be calculated.

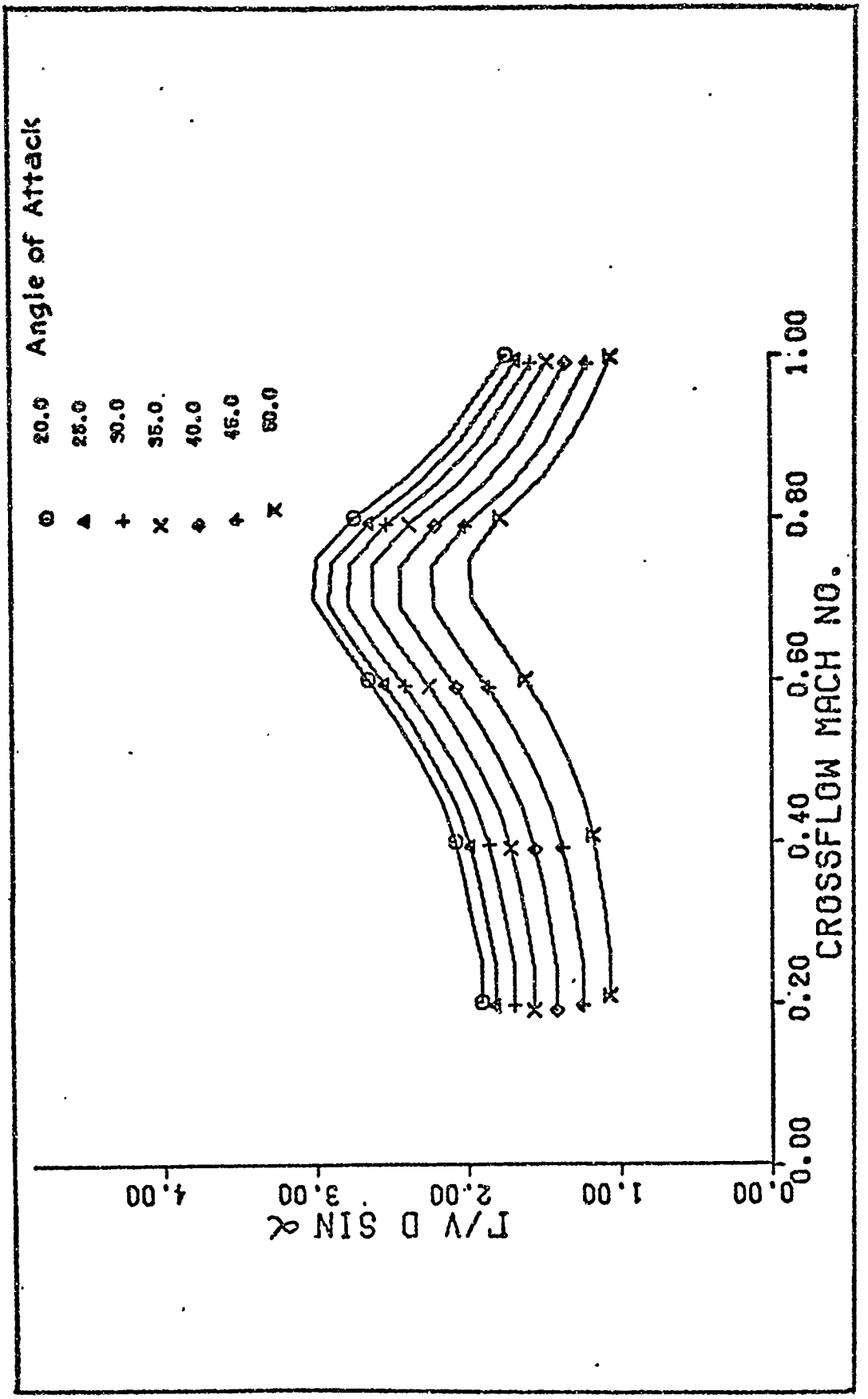

Fig. 9. Vortex Strength Parameter as Function of Crossflow Mach No.

Step 1 Obtain missile geometry, angle of attack (α), and the crossflow Mach number.

Step 2 Determine the Strouhal number from Fig 4.

Step 3 Determine the starting position of the first three vortex lines from Fig 5 if subcritical Reynolds number, or Fig 6 for supercritical Reynolds number. Then determine the starting position of the subsequent vortices using equation

$$g' = \frac{d}{2S \operatorname{Tan} \alpha} \tag{8}$$

Step 4 Determine the angle ξ from Fig 7 and Eq (17).

Step 5 Determine the vortex strength according to

$$\frac{\Gamma}{Vd \sin\alpha} = \coth\left(\sqrt{2}\right)\frac{2}{S}\cos^2\left(\xi\right)\operatorname{Tan}\left(\xi\right)\left(1 - \frac{\operatorname{Tan}\xi}{\operatorname{Tan}\alpha}\right) \tag{15}$$

Step 6 Finally, determine l and h from

$$l = 2g' \operatorname{Tan}\alpha \tag{17}$$

$$h = 2\frac{\sqrt{2}}{\pi} g' \sin\xi \tag{18}$$

Force and Moment Equations

As a result of slender body theory, the transverse force and moments acting on the missile can be calculated if the incompressible two-dimensional potential field for the crossflow plane is known. The potential field for the crossflow plane as a function of distance (X) along the missile body can be related to the two-dimensional unsteady wake development behind a cylinder (Ref 3:643). Thus, if one imagines a plane fixed in the fluid perpendicular to the missile axis, then as the missile pierces this plane, the time required to traverse a distance X along the missile body is given by $t = X/(V \cos\alpha)$, where α is the angle of attack. The

time in the two-dimensional unsteady problem is therefore related to the distance along the missile in the slender body problem.

For the problem of a two-dimensional unsteady wake development behind a cylinder, a force can be calculated as a result of the impulse produced by a pair of vortices of equal and opposite strength Γ, which are a complex distance apart. The instantaneous force per unit length for a system without potential energy is equal to the instantaneous time rate of change of linear momentum. For a vortex pair, the total Kelvin impulse per unit length is equal to the linear momentum (Ref 2:45).

For the 2-D potential flow field in the crossflow plane σ, consisting of a doublet in a free stream (crossflow velocity) and a vortex plus its image as shown in Fig 10, the transverse force equations can be developed.

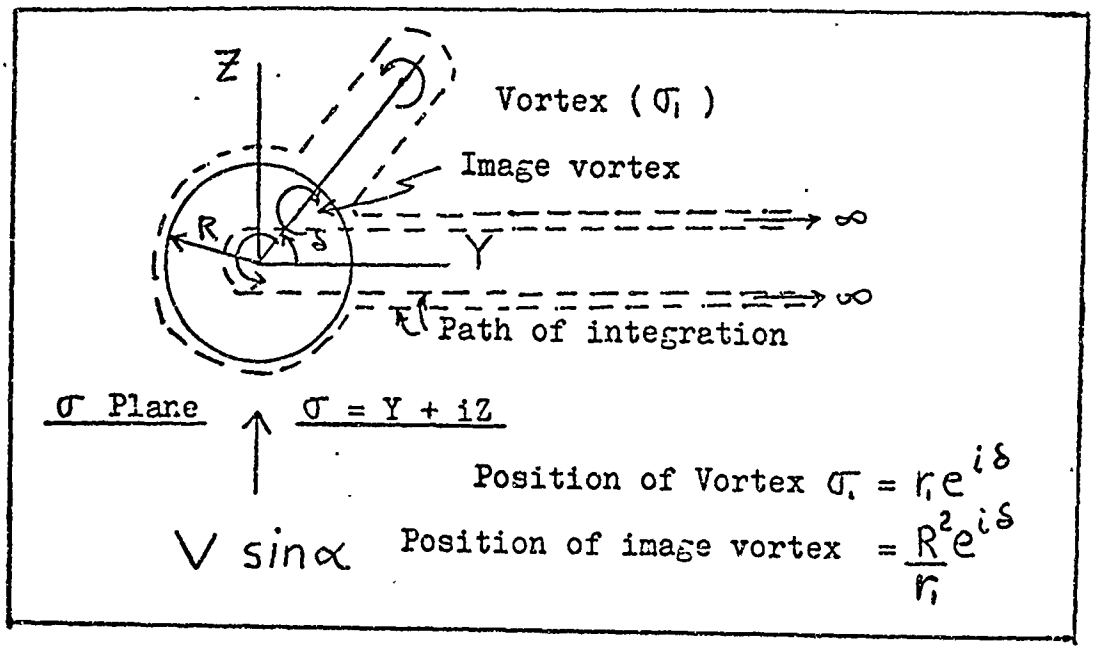

Fig. 10. Crossflow Plane

Transverse Force Equations. Using slender body theory (Ref 2:119-123), the force per unit length acting on the body cross section is equal

to the time rate of change of crossflow momentum vector per unit body length:

$$\frac{d\bar{F}}{dx} = -\frac{d\bar{\zeta}}{dt} \tag{19}$$

where

$$\bar{\zeta} = -\rho \oint \phi \bar{n}\, ds \qquad \text{(momentum vector)}$$

$$\phi(X, Y, Z) = \text{perturbation potential in the } \sigma \text{ plane}$$

$$\bar{V} = V \sin\alpha\, \hat{k} + V \cos\alpha\, \hat{i} + \nabla\phi$$

The integral in the expression for the momentum vector is to be taken around the instantaneous body cross section. Since

$$V \cos\alpha\, dt = dx \tag{20}$$

then,

$$\frac{d\bar{F}}{dx} = \rho V \cos\alpha \frac{d}{dx} \oint_{CB(x)} \phi \bar{n}\, ds \tag{21}$$

By integrating over the body length the total transverse force (normal and yaw) acting on the missile is

$$\bar{F} = \rho V \cos\alpha \oint_{CB(L)} \phi \bar{n}\, ds \tag{22}$$

where CB indicates that the integral is to be evaluated at the base cross section. It is assumed that the initial value of the force is zero and that the integral of the potential along the length of the missile is continuous. If the potential is not continuous along the body of the missile, then the total force must be found as the sum of incremental values. Also, since the force is linear in the perturbation potential, the effect of the addition of more elements in the potential can be found by superposition.

Expressing the force in terms of complex variables and letting

$$\phi' = \phi + V \sin\alpha \, z \tag{23}$$

then

$$\bar{F} = \bar{Y} + i\bar{Z} = -i\rho V \cos\alpha \oint_{CB} \phi' \, d\sigma + i\rho V \cos\alpha \oint_{CB} V \sin\alpha \, z \, d\sigma \tag{24}$$

or

$$\bar{Y} + i\bar{Z} = -i\rho V \cos\alpha \oint_{CB} \phi' d\sigma - i\rho V^2 \cos\alpha \sin\alpha \, \pi R^2 \tag{25}$$

Introducing the complex potential $W'(\sigma)$ for the related flow which has a zero normal velocity at the contour and a velocity at infinity of V sin α, then

$$\bar{Y} + i\bar{Z} = -i\rho V \cos\alpha \oint_{CB} W'(\sigma) \, d\sigma - i\rho V^2 \cos\alpha \sin\alpha \, \pi R^2 \tag{26}$$

where

$$W'(\sigma) = \phi' + i\psi' \tag{27}$$

The potential ϕ' can be replaced by $W'(\sigma)$ since the stream function ψ' is constant along the cross section contour. For the complex potential

$$W'(\sigma) = i V \sin\alpha \left[\sigma - \frac{R^2}{\sigma}\right] - \frac{i\Gamma}{2\pi}\left[\ln(\sigma - \sigma_1) - \ln\left(\sigma - \frac{R^2}{\sigma_1}\right) + \ln\sigma\right] \tag{28}$$

The potential for a missile of circular cross section consists of a doublet in the crossflow stream, a vortex, and its image. Evaluating the contour integral for the path shown in Fig 10 yields

$$\oint_{CB} W'(\sigma)\,d\sigma = 2\pi i\left[-iV\sin\alpha R^2 - \frac{i\Gamma}{2\pi}\left(-\sigma_i + \frac{R^2}{\bar{\sigma}_i}\right)\right] \tag{29}$$

Then the forces are

$$\bar{Y} + i\bar{Z} = i\pi R^2 \rho V^2 \sin\alpha\cos\alpha - i\rho V\cos\alpha\,\Gamma\left[-\sigma_i + \frac{R^2}{\bar{\sigma}_i}\right] \tag{30}$$

or in coefficient form

$$C_Y = \frac{\bar{Y}}{1/2\rho V^2 \pi R^2} = \frac{2\Gamma\cos\alpha}{\pi R^2 V}\, r_i \left[1 - \frac{R^2}{r_i^2}\right]\cos\delta \tag{31}$$

and

$$C_n = \frac{\bar{Z}}{1/2\rho V^2 \pi R^2} = \sin 2\alpha + \frac{2\Gamma\cos\alpha}{\pi R^2 V}\, r_i \left[1 - \frac{R^2}{r_i^2}\right]\sin\delta \tag{32}$$

The small angle approximation has not been made in the above equations. The normal force equation contains two terms, where the $\sin 2\alpha$ is the typical slender body result (if the body is cylindrical) and the other term is due to a vortex and its image. The yaw force equation has a term only due to the vortex and its image. The terms for the vortex forces in the above equations are equivalent to the equations of Nielsen (Ref 10:101).

Moment Equations. In a similar manner, the equations for the moment coefficients can be developed. The moment coefficient equations are

$$C_N = \sum_{i=1} \left(X_i - X_{ref}\right) C_{Yi} \tag{33}$$

and

$$C_M = \sum_{i=1} \left(Y_i - Y_{ref} \right) C_{ni} \tag{34}$$

where the index i indicates the incremental force. The distances are evaluated at selected crossflow planes over the length of the missile.

IV. Comparison of Results

The primary objective of this study was to derive a slender-body mathematical model to predict the forces and moments on a slender missile configuration at angles of attack where asymmetric vortex shedding occurred. Results of these calculations were compared with existing experimental data to test the validity of the mathematical theory.

Experimental data available for comparison of the calculated normal and side force coefficients was obtained from Krouse (Ref 8), Pick (Ref 11), and unpublished data from the Air Force Flight Dynamics Laboratory. Schematic diagrams of the missile configurations tested are shown in Figures 11 and 12, page 34, and Fig 13, page 35. Figures 14-21 (pages 36-43) show the calculated and experimental side force coefficients, and Figures 22-24, pages 44-46, compare normal forces. The first comparisons were made with data obtained by Pick on a small fineness ratio missile configuration. As can be seen in Figures 14, 15, and 16, the side forces agree adequately for angles of attack up to approximately 36-38 degrees. Then, the slender-body model breaks down and the calculated curves depart dramatically from the experimental values. Also, at higher free stream Mach numbers (Fig 17), the calculated values of side force are inaccurate. The slender-body theory, due to compressibility effects, cannot be readily extended to high angles of attack without empirically determined correction factors applied to the model.

Another contributing factor at angles of attack greater than 35 degrees is that g' (the spacing between alternate vortex filaments) decreases in length rapidly as the angle of attack is increased. This shifts the vortex lines forward toward the nose of the missile, and also

causes an increase in the number of filaments which are shed. When an odd number of vortex filaments are shed, the side forces are apparently altered sufficiently that divergence from the predicted results occurs.

Results from models of high missile fineness ratio are plotted in Fig 18 (Model #3), Figures 19 and 20 (Model #4), and Fig 21 (Model #5); consequently, many vortex filaments are shed due to the increased missile body length. It was found that at the higher free stream Mach numbers the calculated values of side force (Figures 20 and 21) tend to display discontinuities.

The plots in Fig 20 were determined by shifting the starting positions of the vortex lines along the missile body axis to show the sensitivity that results. Each succeeding vortex filament sheds on opposite sides of the missile; consequently, the side forces induced on the missile are of opposite sense. Also, a shift in the starting position of the vortex lines can alter the total number of vortex filaments shed which can result in a change of the total induced side force. However, the total normal force is less sensitive to this shift because each left and right handed filament always produces a positive normal force.

The final set of data was obtained from Krouse (Ref 8) from a free stream Mach number of 0.55 and 0.8. Krouse divided the absolute values of the side force coefficient by the lift coefficient and plotted these values versus the angle of attack. Krouse measured side forces that were approximately 60-70 per cent as large as the lift force on his tunnel model. The results are plotted in Fig 18. Krouse's model displayed similar characteristics for a high missile fineness ratio model.

The normal force distribution (lift), which includes a term from slender-body theory, gives reasonably accurate results when compared with

experimental data as shown in Figures 22-24. Again, at the higher angles of attack (greater than 40 degrees) and at greater free stream Mach numbers, the extension of the slender-body model becomes inadequate. Shock waves in the flow field are evidently weak until the crossflow Mach number exceeds about 0.7. Below this value, the drag is predominately due to the wake vortices, but wave drag becomes progressively more important for high Mach numbers.

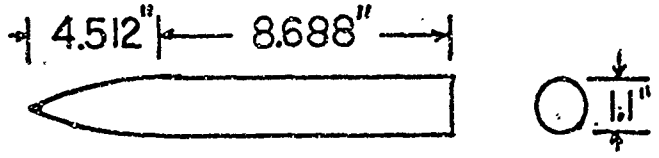

Model #1. 5% Bluntness. FR = 12
Re = 2.7 X 10^6 to 4.3 X 10^6

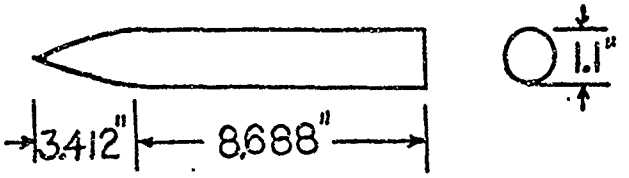

Model #2. 5% Bluntness. FR = 11
Re = 2.7 X 10^6 to 4.3 X 10^6

Fig. 11. Ogive-Missile Configuration from Pick (Ref 11:8)

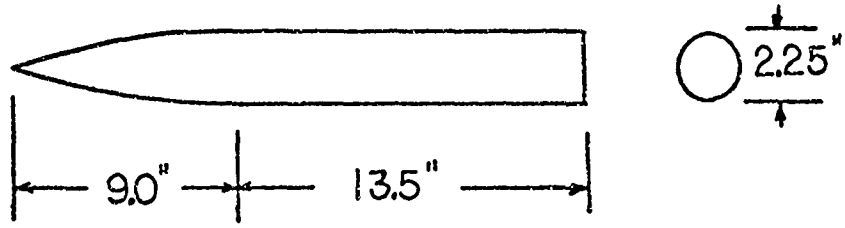

Model #3. FR = 10 Re = 0.7 X 10^6

Fig. 12. Ogive-Missile Configuration from Krouse (Ref 8:11)

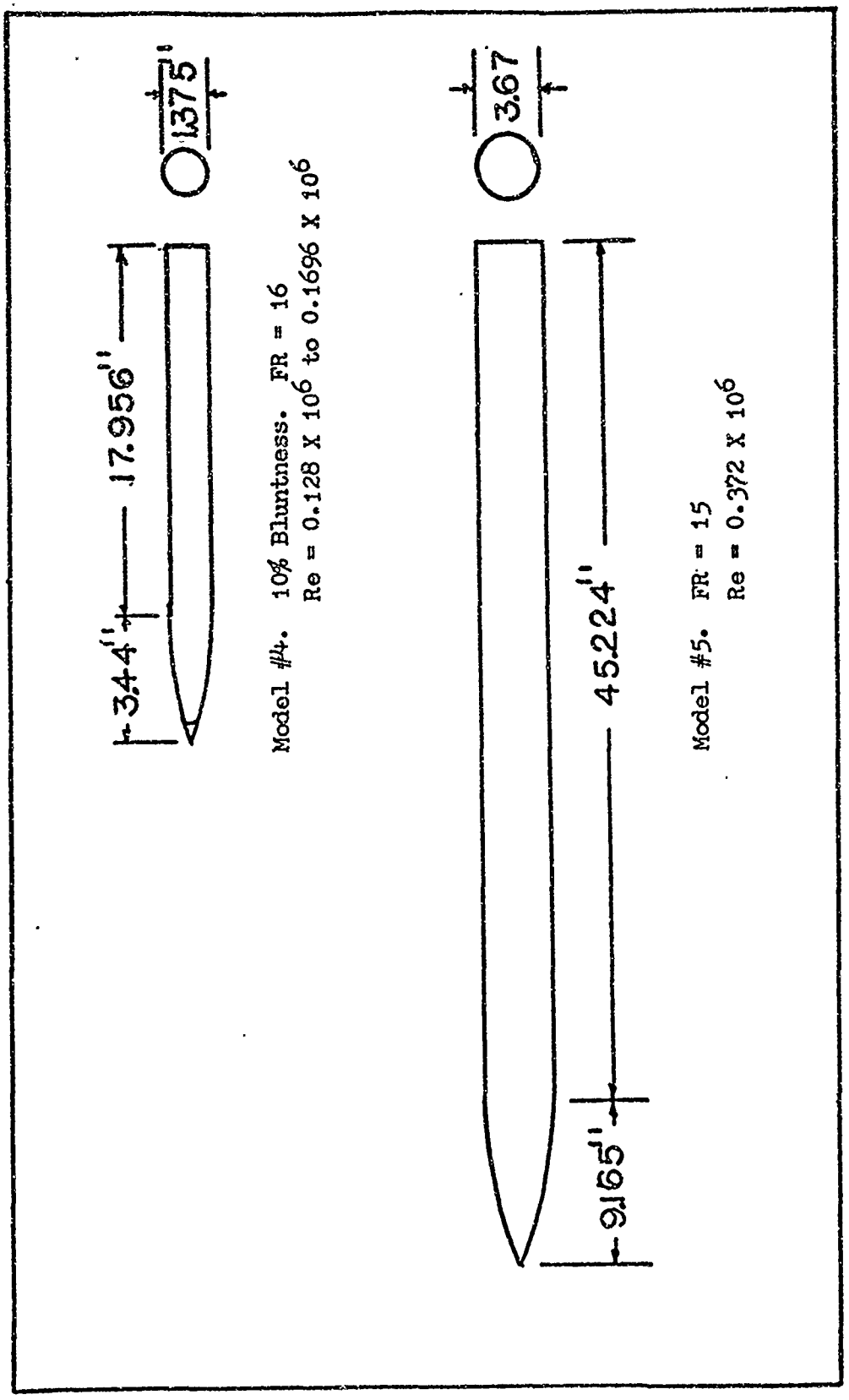

Fig. 13. Ogive-Missile Configuration from the Air Force Flight Dynamics Laboratory

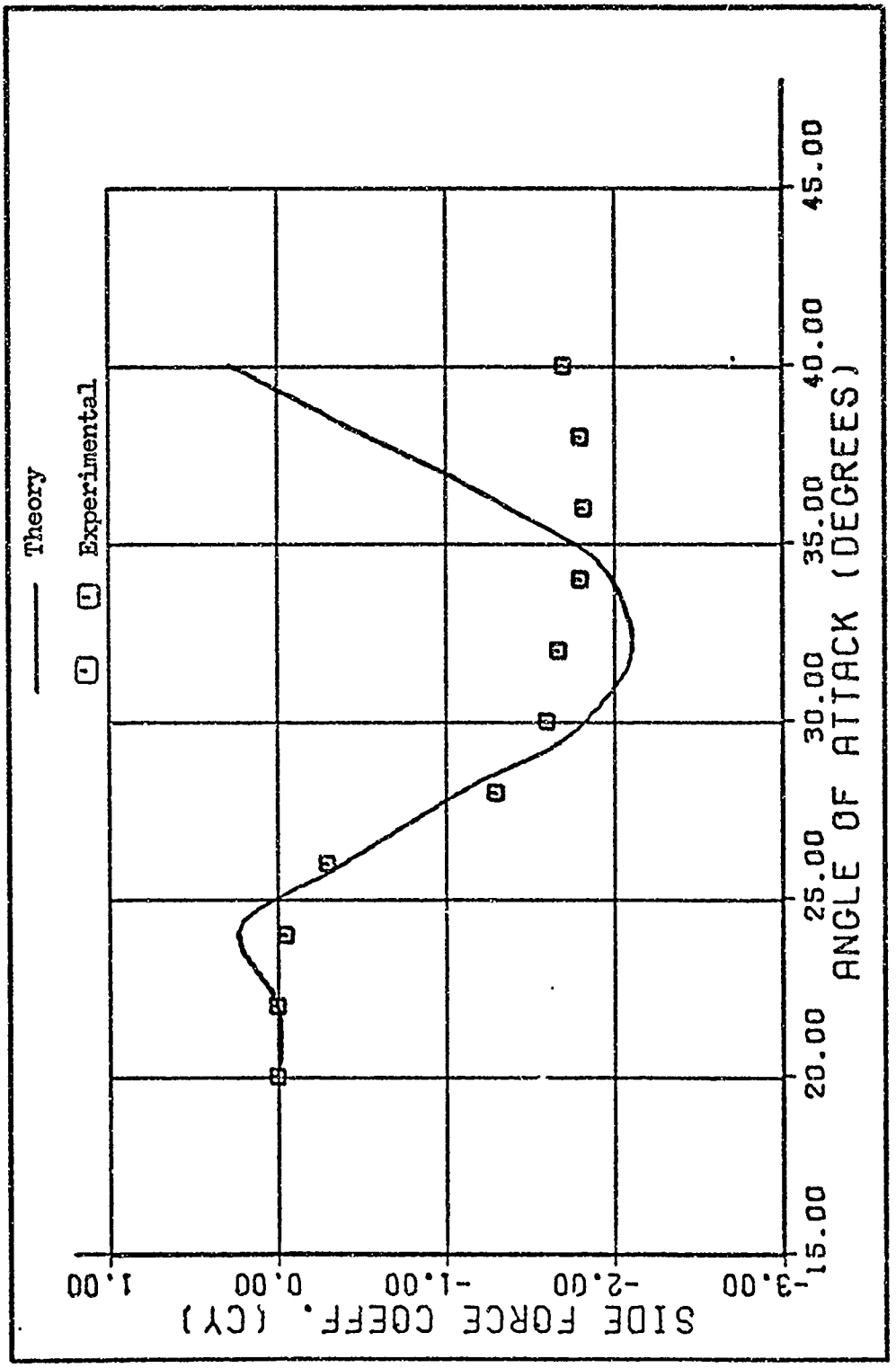

Fig. 14. Model #1. Side Force Coefficient Vs Angle of Attack for Free Stream Mach No. = 0.5

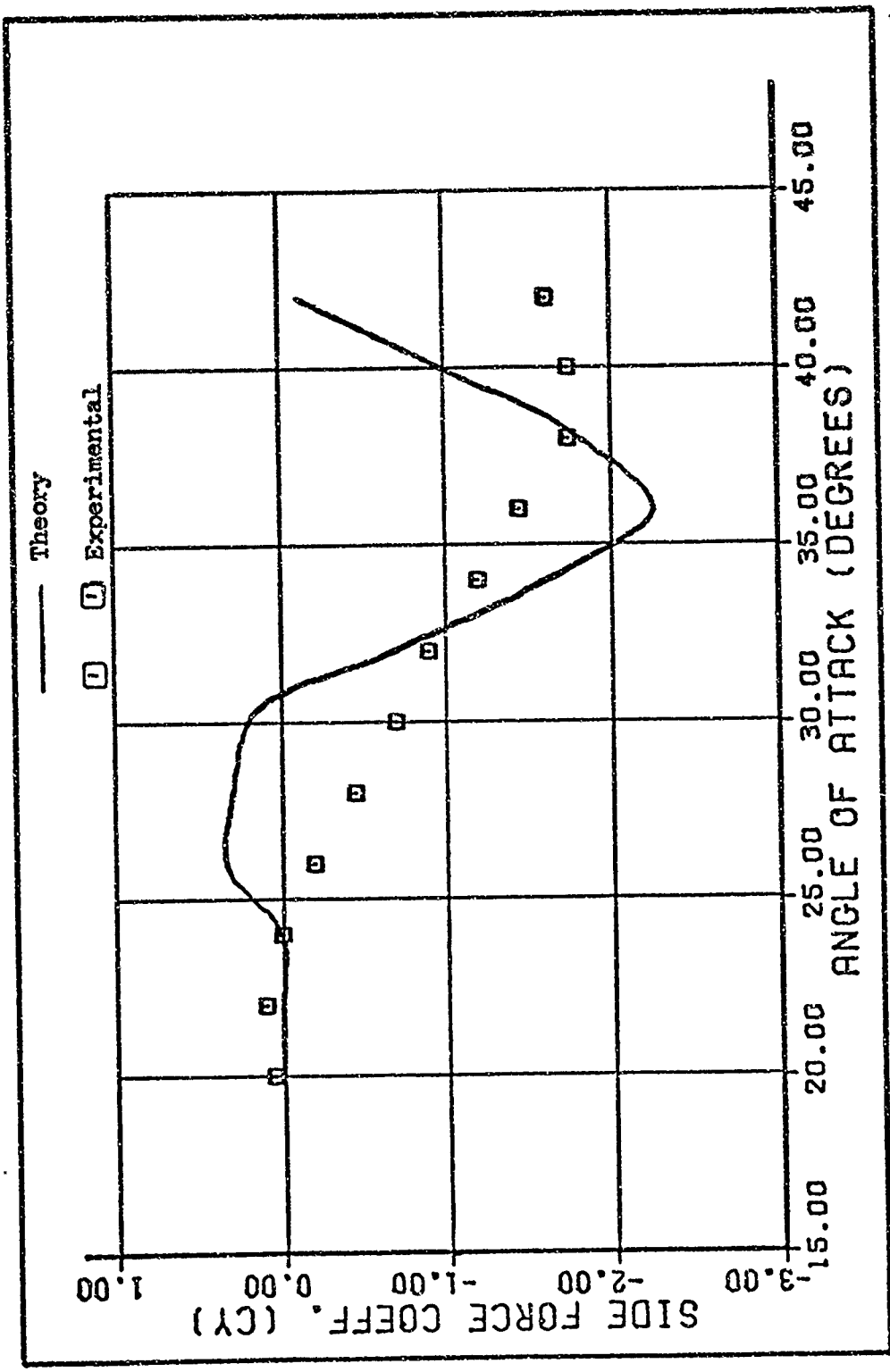

Fig. 15. Model #1. Side Force Coefficient Vs Angle of Attack for Free Stream Mach No. = 0.6

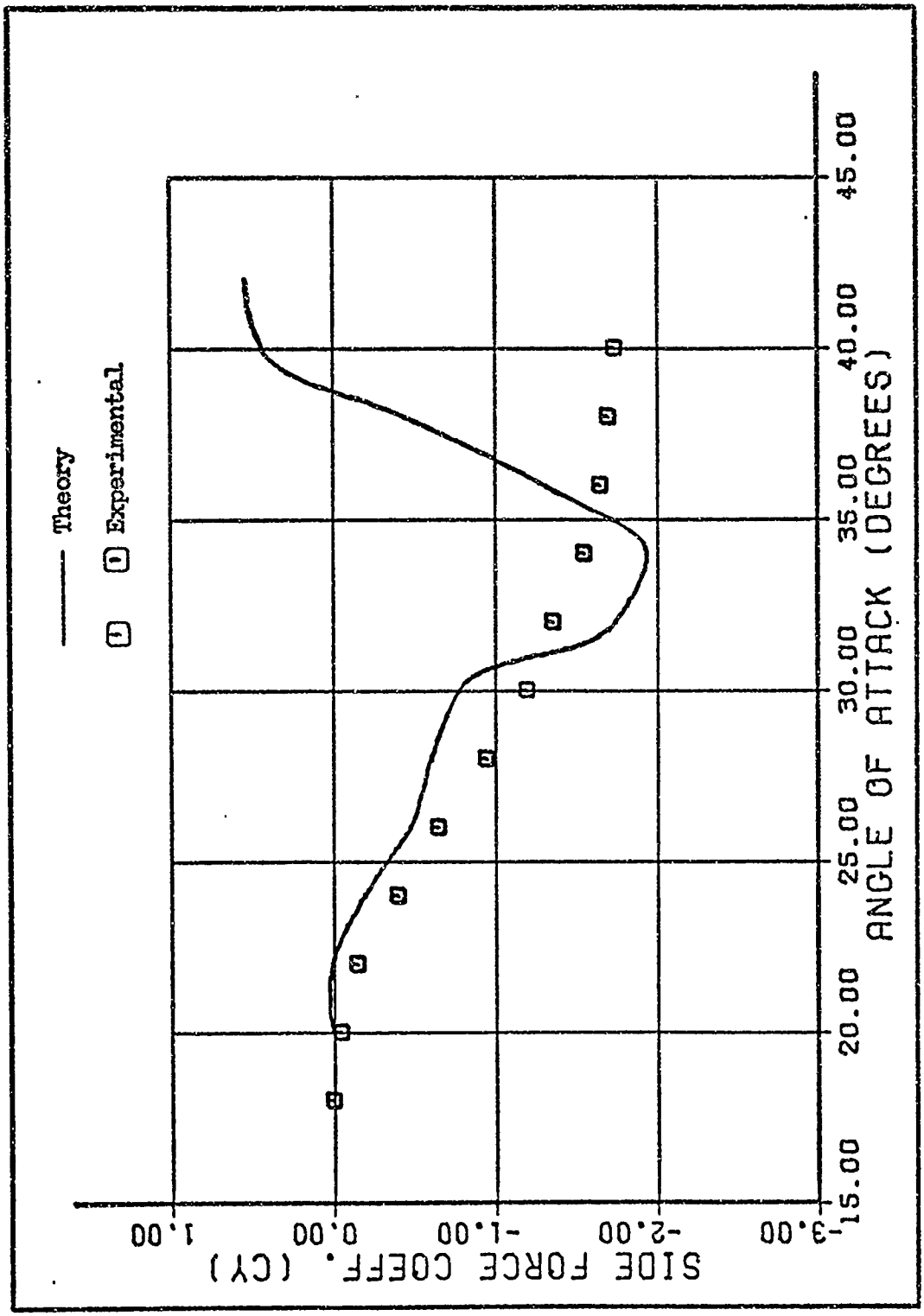

Fig. 16. Model #2. Side Force Coefficient Vs Angle of Attack for Free Stream Mach No. = 0.6

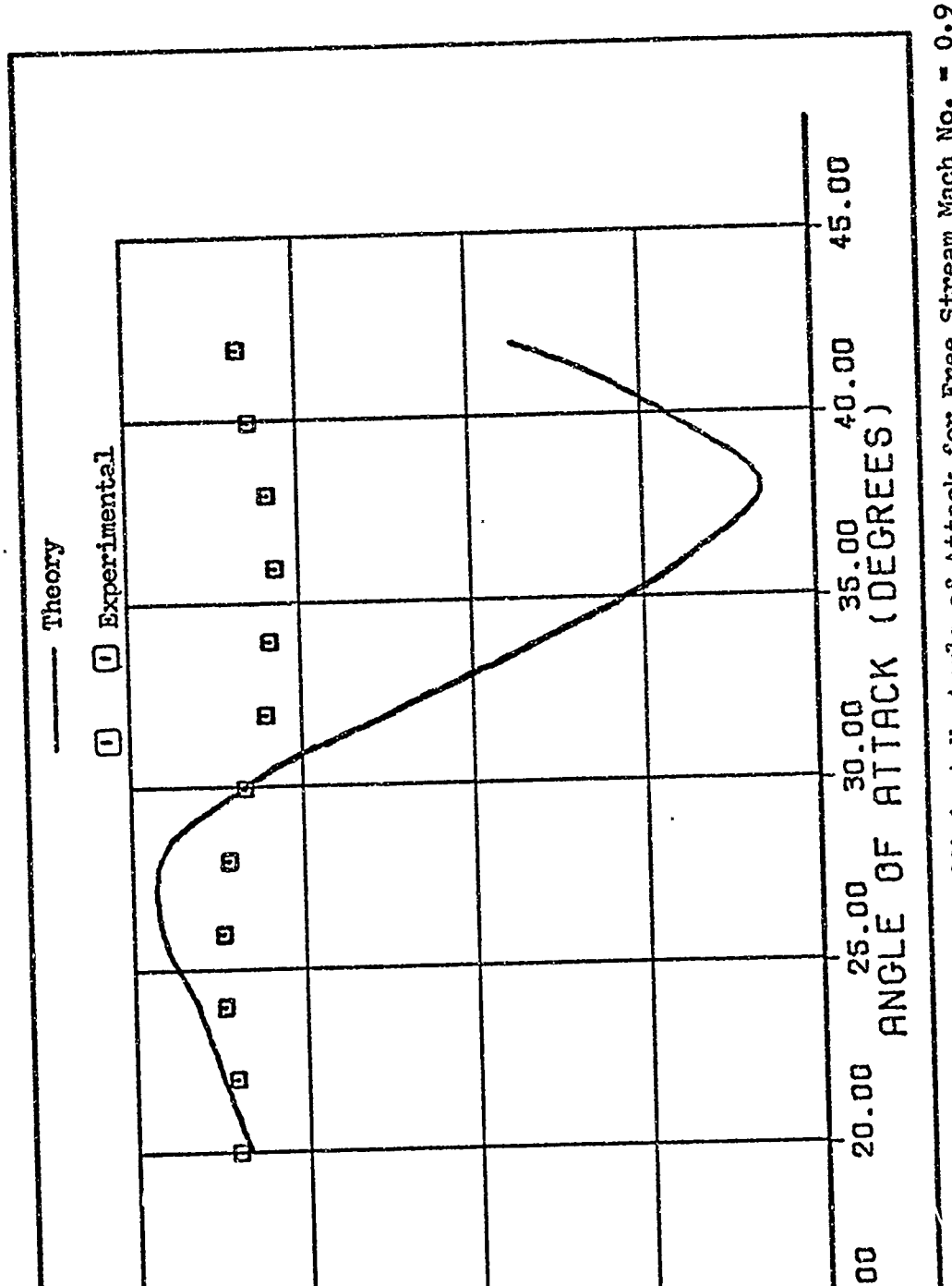

Fig. 17. Model # 2. Side Force Coefficient Vs Angle of Attack for Free Stream Mach No. = 0.9

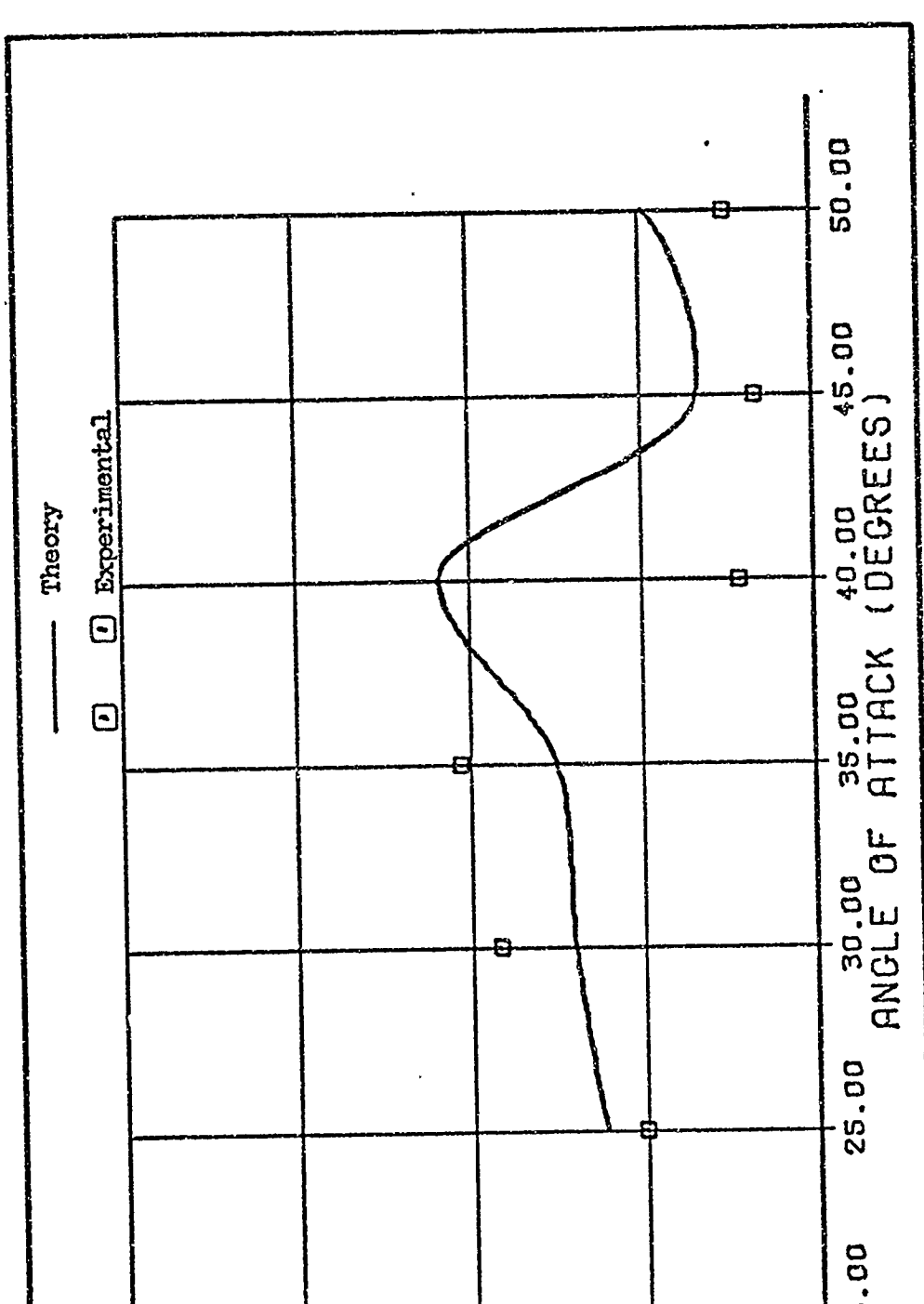

Fig. 18. Model #3. Absolute Side Force Coefficient Divided by the Lift Coefficient Vs Angle of Attack for Free Stream Mach No. = 0.55

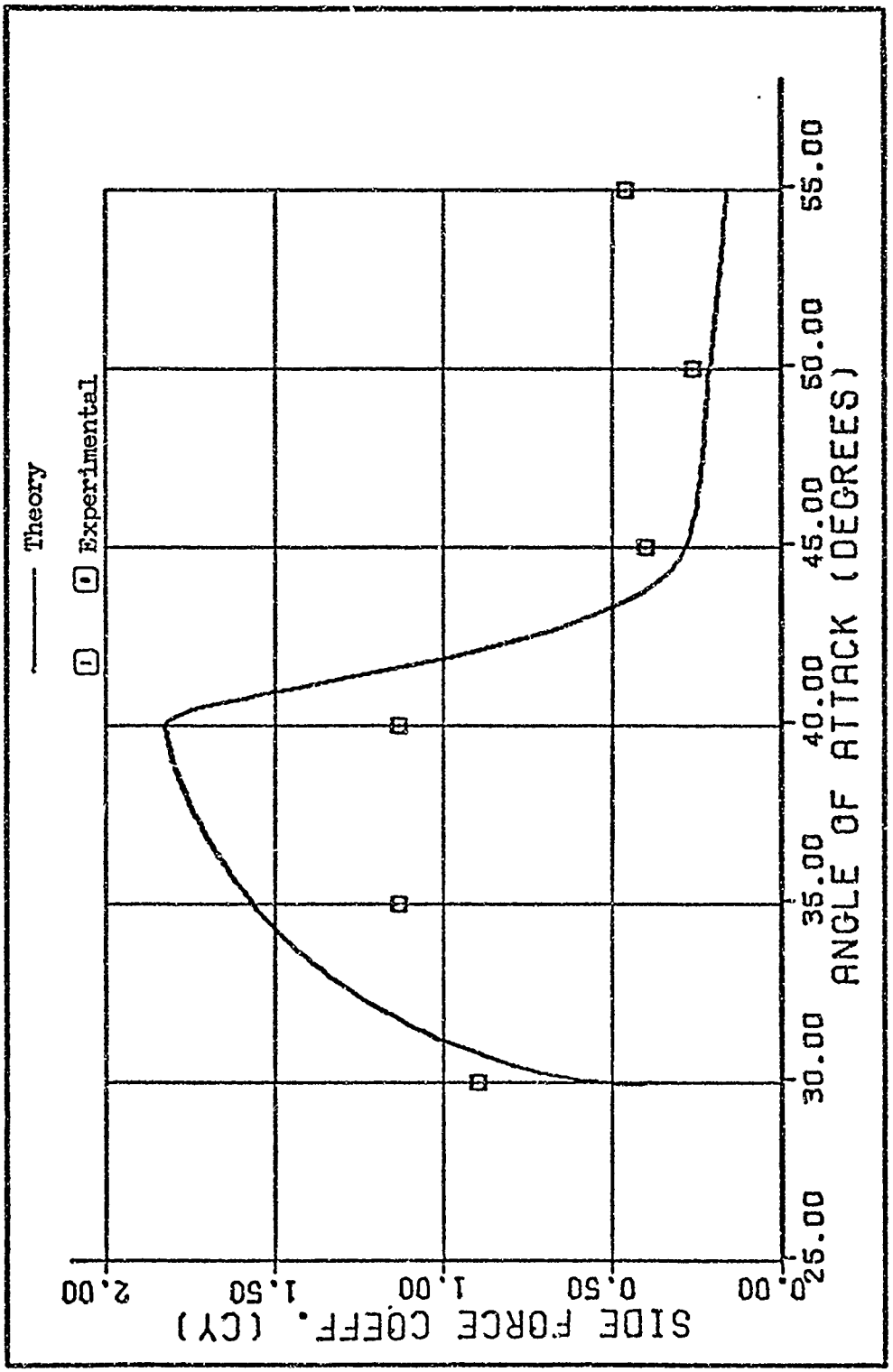

Fig. 19. Model #4. Side Force Coefficient Vs Angle of Attack for Free Stream Mach No. = 0.6

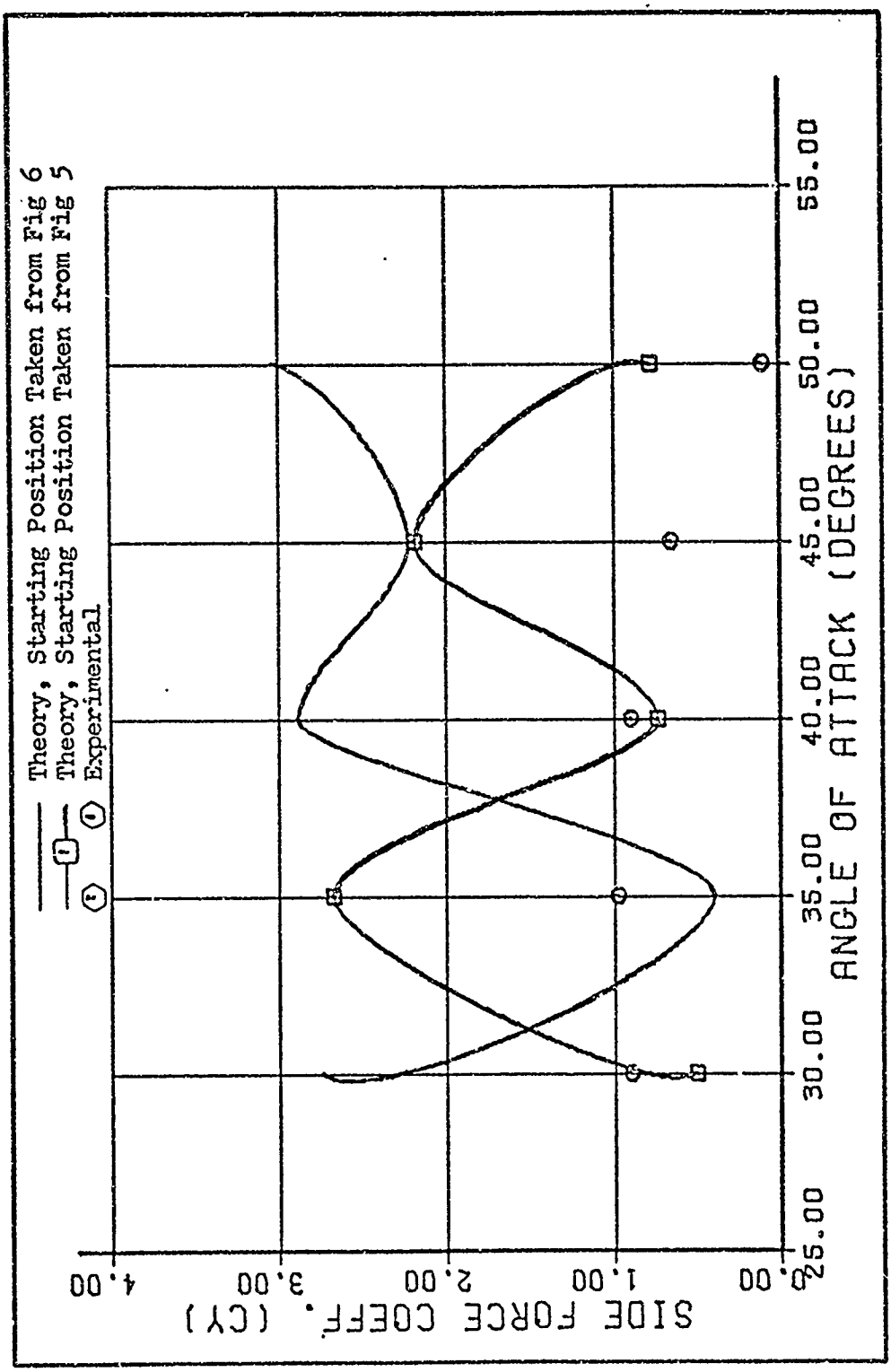

Fig. 20. Model #4. Side Force Coefficient Vs Angle of Attack for Two Different Starting Positions for the Vortex Filaments at Free Stream Mach No. = 0.85

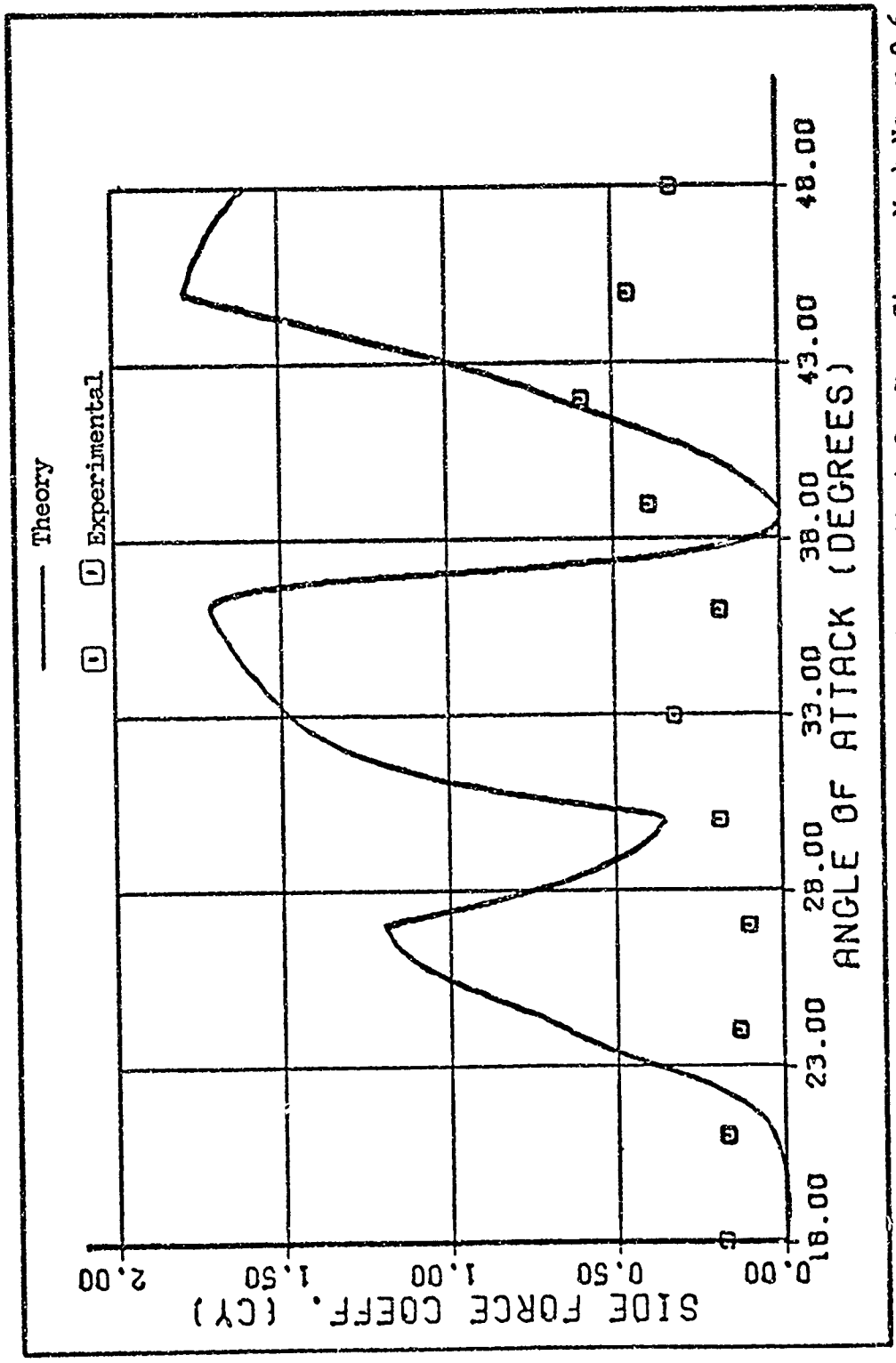

Fig. 21. Model #5. Side Force Coefficient Vs Angle of Attack for Free Stream Mach No. = 0.6

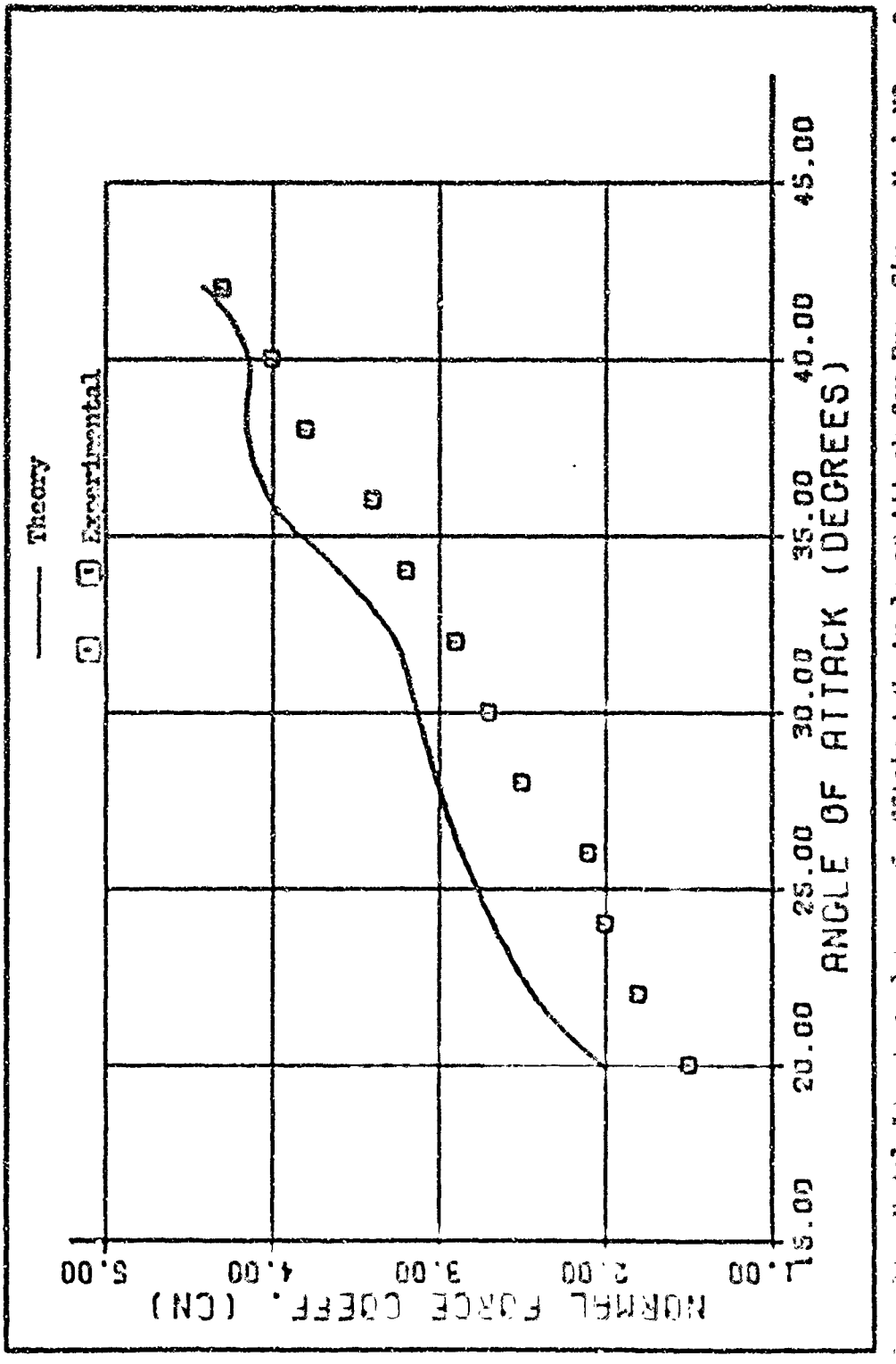

Fig. 24. Model #2. Normal Force Coefficient Vs Angle of Attack for Free Stream Mach NO. = 0.6

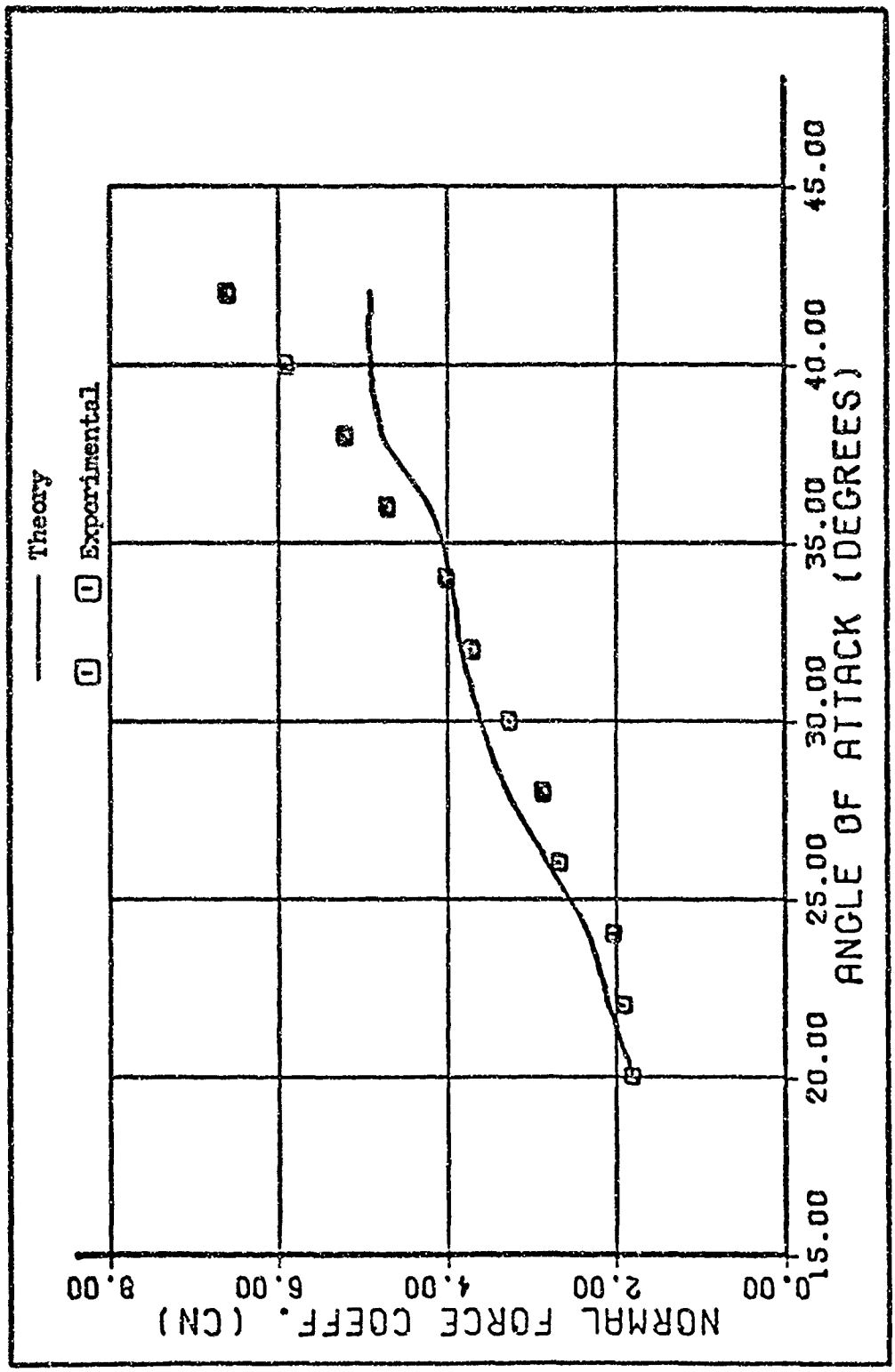

Fig. 23. Model #2. Normal Force Coefficient Vs Angle of Attack for Free Stream Mach No. = 0.9

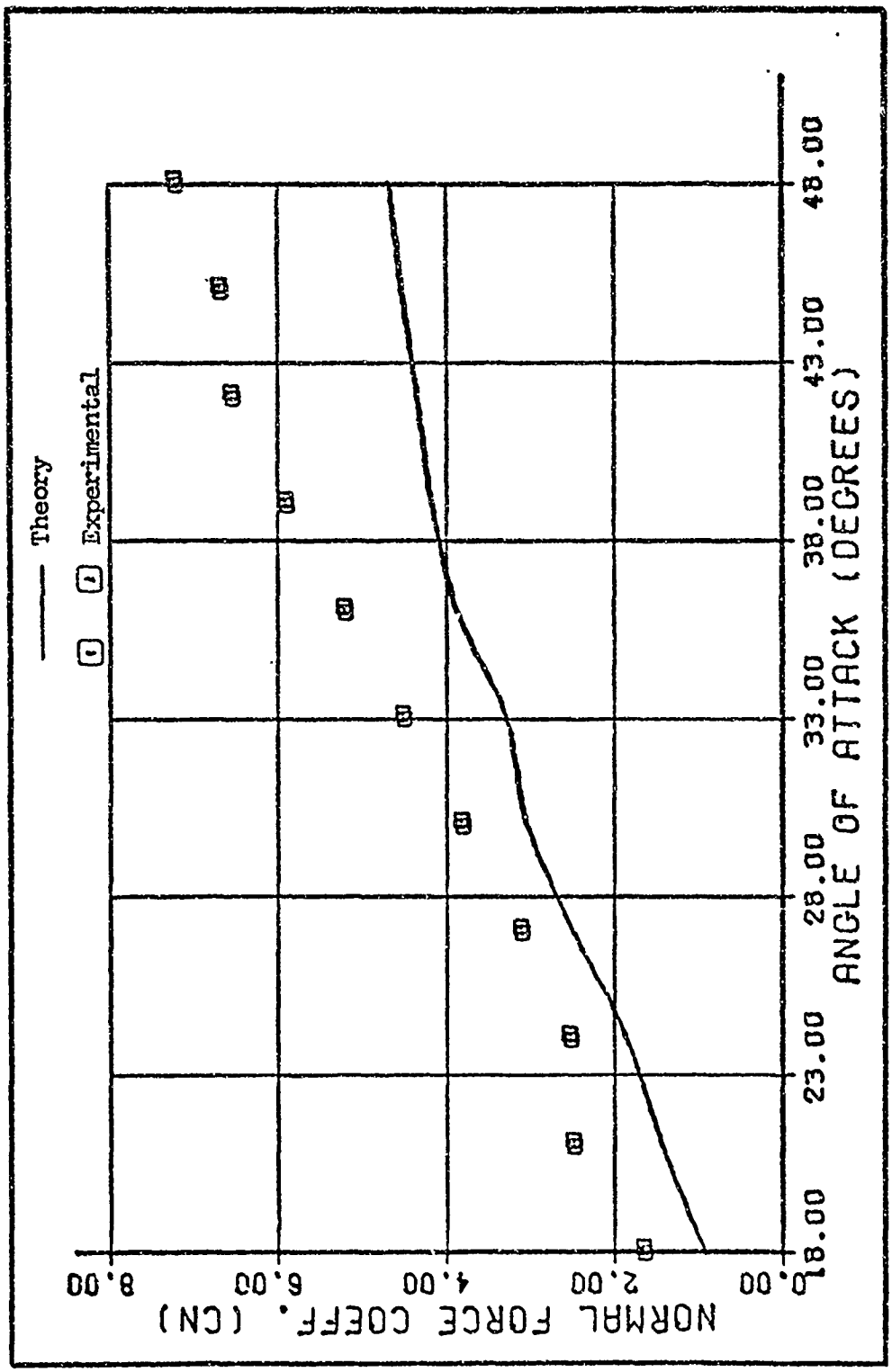

Fig. 24. Model #5. Normal Force Coefficient Vs Angle of Attack for a Free Stream Mach No. = 0.6

V. Conclusions

a. The mathematical model is extremely sensitive to the angle of attack, free stream Mach number, and missile fineness ratio.

b. Any mathematical model will have to rely heavily upon experimental data to determine the starting positions and vortex strengths of the shed vortex sheets. The model used in this report assumed a constant vortex strength; however, if the last filament has not fully developed, the strength will not be the same.

c. The model predicts the trend of the side forces adequately for low Mach numbers and low missile fineness ratios, but as the fineness ratio or free stream Mach number increases, the predicted results become inadequate.

d. The normal force predictions are relatively accurate within the angle of attack and Mach number regimes studied in this report.

e. The sensitivity of the starting position of the vortex filaments has a dramatic effect upon the calculated side force coefficients.

f. The accurate prediction of the starting positions of the first two vortex filaments is necessary for various nose geometries and missile fineness ratios.

g. The contribution of the wake formation due to the nose section of the missile is not understood; however, Pick (Ref 11) has shown that a turbulent boundary layer reduces the magnitude of the side force considerably. Thus, an effective way to minimize the side force effect is to use small fineness ratio or high bluntness ratio nose sections and induce a turbulent boundary layer on the surface.

V. Conclusions

a. The mathematical model is extremely sensitive to the angle of attack, free stream Mach number, and missile fineness ratio.

b. Any mathematical model will have to rely heavily upon experimental data to determine the starting positions and vortex strengths of the shed vortex sheets. The model used in this report assumed a constant vortex strength; however, if the last filament has not fully developed, the strength will not be the same.

c. The model predicts the trend of the side forces adequately for low Mach numbers and low missile fineness ratios, but as the fineness ratio or free stream Mach number increases, the predicted results become inadequate.

d. The normal force predictions are relatively accurate within the angle of attack and Mach number regimes studied in this report.

e. The sensitivity of the starting position of the vortex filaments has a dramatic effect upon the calculated side force coefficients.

f. The accurate prediction of the starting positions of the first two vortex filaments is necessary for various nose geometries and missile fineness ratios.

g. The contribution of the wake formation due to the nose section of the missile is not understood; however, Pick (Ref 11) has shown that a turbulent boundary layer reduces the magnitude of the side force considerably. Thus, an effective way to minimize the side force effect is to use small fineness ratio or high bluntness ratio nose sections and induce a turbulent boundary layer on the surface.

h. The discrepancies at the higher Mach numbers are due to the unknown size of the wave drag which is produced by shock waves in the flow.

Unfortunately, there is little quantitative experimental data available to determine the root causes and effects of asymmetrical vortex wakes behind a missile in the Mach number and Reynolds number regimes investigated in this report. Therefore, the validity of the theory and subsequent developed mathematical model cannot be completely verified. The results obtained indicated that the method yields reasonable results for low fineness ratio missile configuration for angles of attack (α) up to 40 degrees. Based on the success for the low fineness ratio missile configurations, the model might be extended to higher fineness ratio missiles, provided suitable experimental data become available to permit empirical prediction of the location of the vortex separation points.

VI. Recommendations

The problem of asymmetric vortex shedding definitely warrants further investigation since there are many unanswered questions concerning the stability and control of a missile which may operate at large angles of attack.

At this time there are no analytical techniques for quantitatively describing the side forces and yawing moments induced on a slender missile at relatively high angles of attack. Therefore, the proposed model, which was based upon slender-body theory and vortex street analysis, could possibly be refined for various missile configurations provided a systematic study is made to determine:

a. The effects of nose bluntness, fineness ratio, and overall missile fineness ratio on the starting position of the vortex filaments

b. Whether at subsonic free stream flight speeds, some type of equivalent Kutta condition, which influences the breakaway position of the vortex filaments, prevails at the base of a finite missile

c. The angle of attack ranges and free stream Mach numbers which characterize a particular wake flow phenomena (steady, unsteady, symmetric, asymmetric, and/or turbulent)

d. If the diameter of an aft-mounted sting, which has nearly the same diameter as that of the tunnel model being tested, alters the flow field significantly since the missile now has a higher fineness ratio than the simulated free-flight model

e. The accuracy of the circulation strength of the vortex filaments

f. The effects of the vortex induced flow field on the roll moment above what is normally experienced on a finned missile configuration

Bibliography

1. Allen, H. J. and Perkins, E. W. A Study of Effects of Viscosity on Flow Over Slender Inclined Bodies of Revolution. NACA TR No. 1048 (1951).

2. Ashley, H. and Landahl, M. Aerodynamics of Wings and Bodies. New York: Addison-Wesley Publishing Co., Inc. (1965).

3. Bryson, A. E. "Symmetric Vortex Separation on Circular Cylinders and Cones." ASME Journal of Applied Mechanics, 26:643-648, (1959).

4. Clark, William H. and Peoples, John R. "Occurrence and Inhibition of Large Yawing Moments During High Incidence Flight of Slender Missile Configuration." AIAA Paper No. 72-968 (September 1972).

5. Fung, Y. C. "Fluctuating Lift and Drag Acting on a Cylinder in a Flow at Supercritical Reynolds Numbers." Journal of the Aerospace Science, 27:801 (1960).

6. Goldstein, S. Modern Developments in Fluid Dynamics. New York:Dover Publishing, Inc., Vol I (1964).

7. Griss, R. J. "Velocity Traverse in the Wake of a Yawed Cylinder." ARL Aerodynamic Technical Memorandum No. 230 (1967).

8. Krouse, J. R. "Induced Side Forces on Slender Bodies at High Angles of Attack and Mach Numbers of 0155 to 018." NSRDC Test Report No. A1-79 (1971).

9. Milne-Thomson, L. M. Theoretical Hydrodynamics. New York: MacMillan Co.(1960).

10. Nielsen, Jack N. Missile Aerodynamics. New York: McGraw-Hill Book Co., Inc.(1960).

11. Pick, G. S. "Investigation of Side Forces on Ogive Cylinder Bodies at High Angles of Attack in the M = 0.5 to 1.1 Range." AIAA 4th Fluids and Plasma Dynamics Conference. No. 71-570 (1971).

12. Schindel, L. H. "Effect of Vortex Separation on the Lift Distribution on Bodies of Elliptic Cross Section." Journal of Aircraft, 6:537-543 (1969).

13. Thomson, K. D. and Morrison, D. F. "The Spacing, Position and Strength of Vortices in the Wake of Slender Cylindrical Bodies at Large Incidence." Journal of Fluid Mechanics, 50:751-783 (1971).

14. Thomson, K. D. and Morrison, D. F. "The Spacing, Position and Strength of Vortices in the Wake of Slender Cylindrical Bodies at Large Incidence." Australian Department of Supply, WRE Report HSA25 (1969).

Vita

Major John S. Kubin was born on [redacted] in [redacted], the son of Stanley C. and Rose E. Kubin. After graduation from Crosby High School in 1954, he enrolled at Texas A & M University. In January 1959, he graduated with a degree of Bachelor of Science in Mechanical Engineering and was awarded a commission as a Second Lieutenant in the United States Air Force Reserves. He began flight training upon entering active duty in April 1959, and subsequently graduated as a USAF Pilot in June 1960.

Prior to coming to the Air Force Institute of Technology in June 1972, his Air Force assignments included: five years as an Instructor Pilot at Webb AFB, Big Spring, Texas; a year's flying combat tour at Tan Son Nhut AB, Republic of South Vietnam; three years on the 26th Tactical Recon Wing Staff at Ramstein AB, Germany; and three years as a Strategic Air Command KC-135 Pilot/Instructor-Pilot at Barksdale AFB, Louisiana.

Permanent address: [redacted]

This thesis was typed by Betty Armentrout.